CSIRO

MINERALS RESEARCH LABORATORIES

FUEL GEOSCIENCE UNIT

RESEARCH ON TASMANITE OIL SHALE

- THIRD QUARTERLY REPORT TO ENDEAVOUR RESOURCES LIMITED

A. TELFER, N.J. RUSSELL, R.P. PHILP AND J.D. SAXBY

P.O. Box 136

NORTH RYDE, NSW

AUSTRALIA 2113

JULY 1979

001

146002

CONTENTS

002

TABLES

003

FIGURES

1. SUMMARY

1. Further research on the Tasmanite shale has been carried out in the fields of chemical isolation and characterization of kerogen, petrology of separated kerogen, and hydrogenation and flash pyrolysis of a kerogen concentrate.

2. The atomic H/C ratio of isolated tasmanite kerogen is 1.60, while the atomic O/C ratio is 0.02. High H/C values and low O/C values such as these are desirable for any process leading to liquid products.

3. The high organic sulphur content of Tasmanite kerogen (∿ 4%) is probably due to the presence of -S- and -S-S- groups and will be a problem in any conversion process. No simple way of overcoming this adverse feature is available due to the nature and uniform distribution of these chemical groups.

4. Environmentally hazardous trace metals do not appear to be concentrated in the Tasmanite kerogen.

5. For this type of material flash pyrolysis to liquid and gaseous products is unlikely to have any advantage over slower pyrolytic methods.

6. The compositions of gas samples from batch autoclave studies reflect the differences between the uncatalysed experiments, which are dominated by thermal breakdown reactions, and the catalysed experiments, which are dominated by thermocatalytic reactions at the lower reaction temperatures.

7. Changes in the optical behaviour of the alginite in response to an increase in the reaction temperature suggest that tin(II) chloride inhibits the decrease in alginite fluorescence intensity, whereas zinc(II) chloride enhances the decrease in alginite fluorescence intensity. This suggests that these catalysts produce different types of hydrogenation reaction.

8. Irrespective of the experimental conditions, similar maximum yields of heavy hydrocarbons are generated between 425°C and 450°C. This reflects the fact that the alginite is rich in alkane precursors, e.g. fatty acids, etc.

2. INTRODUCTION

This is the third quarterly report for Endeavour Resources Limited on the Tasmanite Oil Shale Project. It contains details of work completed since the second report in April 1979 (IR 1016R).

The continuing assessment of the tasmanite shale has been dominated, this quarter, by examinations carried out on two samples: the kerogen concentrate (LN 77591), supplied by the company, and an average grade sample from China Flat - Bore No. 13B, 70'8½"-75'10" (21.6-23.1 m), LN 78694.

Small-scale demineralization was carried out on the two samples to give organic materials virtually free of diluting mineral matter and suitable for precise petrological and chemical characterization. The demineralised samples were chemically analysed by proximate, elemental and micro methods for comparison with the original samples.

Microscopic examination was undertaken to examine the effect of demineralization on the algal bodies and the effectiveness of reducing ash content by way of mineral elimination. X-ray diffraction techniques were used to determine the composition of the resistant mineral matter.

Carbonization and hydrogenation of the kerogen concentrate under pressure (LN 77591) were carried out both in the presence and absence of catalysts. This involved the running of four parallel series of experiments at a number of reaction temperatures. Samples of the concentrate were heated, under pressure in (i) nitrogen (carbonization); (ii) hydrogen (uncatalysed hydrogenation); (iii) hydrogen and tin(II) chloride (catalysed hydrogenation); and (iv) under hydrogen and zinc(II) chloride (catalysed hydrogenation). The solid products of these tests were examined under the microscope. Gaseous and liquid products were also analysed and compared.

The kerogen concentrate (LN 77591) was also subjected to flash pyrolysis for estimation of oil and char yields by this technique.

Hydrogenation studies were carried out and analysed by N.J. Russell Curie point pyrolysis by R.P. Philp and petrological and chemical work by A. Telfer and J.D. Saxby.

3. CHEMICAL AND PETROLOGICAL CHARACTERIZATION OF TASMANITE KEROGEN

Since the mineral matter content of all the shale samples examined so far is quite high, it is necessary to isolate the organic matter (kerogen) from such samples before accurate data characterizing the kerogen can be obtained. The Tasmanite concentrate supplied by Endeavour Resources still contains over 30% mineral matter and so even in this case, further removal of inorganic minerals is needed. Thus, the following samples were chosen for demineralization:

Lab. No. 77591: flotation concentrate
Lab. No. 78694: core from Bore 13B (21.6-23.1 m) (China Flat area)

Demineralization was achieved by the use of acids to remove carbonates and silicates, as follows; (1) dilute hydrochloric acid is mixed with the crushed tasmanite samples, and heated. This is repeated until no further noticeable reaction occurs; (ii) concentrated hydrofluoric acid is added, the sample is again heated, over a water bath, then allowed to cool and settle. After settling, excess liquid is pipetted off, and the sample washed with distilled water until it is no longer acidic. The sample is then dried and weighed. This whole process is repeated until the sample loses no more than approximately 5% of the total weight.

Details of the chemical demineralizations, which were carried out quantitatively taking great care with washing and drying, are given in Table 1. In each case the final kerogens were dried at 105°C in vacuo and analysed by micro-methods for carbon, hydrogen, nitrogen, sulphur, ash, fluorine, chlorine and iron. By making the following assumptions the elemental composition of the kerogen has been derived (Table 2):

(i) All iron is taken to be present as pyrite (FeS_2)
(ii) All non-pyritic sulphur is assumed to be organic sulphur
(iii) Chlorine and fluorine contents are taken to be due to adsorbed HCl and HF.

X-ray diffraction analysis of the powdered kerogens was also carried out (Fig. 1). This confirmed the absence of pyrite in 77591KK and its presence in 78694KK. It appears that the occurrence of pyrite is dependent on sample location or that the flotation procedure used to obtain the concentrate is very effective in eliminating pyrite. The X-ray

diffraction traces confirm that no valuable chemically-resistant trace minerals are concentrated in the kerogens. In the case of 78694KK only small amounts of rutile (and possibly zircon) were detected. The broad organic peak is centered at 4.5-4.7Å in both samples. This value is consistent with essentially aliphatic kerogen having some cross-linking sulphur groups and is different from the aromatic peak usually found for coals at 3.4-3.6 Å.

Trace element analysis by emission spectroscopy was carried out on the two kerogens. This was a continuation of previous trace metal studies (IR 1016R) aimed at finding whether any environmentally hazardous metals are organically bound in Tasmanite. No such metals are apparent from the data in Table 3 and indeed most of the trace metals present are probably contained in the small amount of mineral matter not removed during HCl/HF treatment.

Petrology. Samples 77591K and 78694K were mounted in polished blocks and examined petrologically (See Table 4).

Overall the demineralization treatment proved efficient in completely eliminating clays and metal carbonates from the two samples. Sample LN 77591 originally contained 12% clay and trace carbonate, and sample LN 78694 had 46% clay and 2% carbonate. The quartz content of both was reduced by approximately 1% and 11% respectively. Pyrite still remains, as this is unaffected by these acids. The algal bodies themselves also show no affect from the acids.

Both samples contain whole or fragmental algal bodies varying in size. The majority of the material has formed into clumps. This appears to result from the chemical treatment of the material. The pyrite, which is predominantly small-grained, from <2 up to 5 microns, also congreates in these algal body clumps, especially in sample 78694K. There is little framboidal pyrite remaining.

This clumping is a problem in accurate petrological examination and would also be disadvantageous if it occurred in any physical beneficiation of Tasmanite. This may especially be so in flotation, if the pyrite grains remain in the clumps in the floated fraction, preventing separation of that mineral matter.

The following conclusions can be drawn from the demineralization of Tasmanite and the petrology and elemental composition of the resulting kerogen.

(i) Chemical demineralization effectively removes most mineral matter (except pyrite) and has no visible effect on the organic matter composing the algal bodies.

(ii) Kerogens from the two samples are very similar chemically and petrologically. This is despite the fact that the flotation concentrate contains mainly large algal bodies, while the China Flat sample contains a proportion of finely dispersed organic matter.

(iii) The organic sulphur content of Tasmanite is $\gtrsim$ 4% and is presumably present as cross-linking -S-S- and -S- groups.

(iv) The atomic H/C ratio of the kerogen is high (1,60), while the O/C ratio is low (0,02). The small oxygen content is advantageous from the point of view of producing oils by pyrolysis requiring a minimum of subsequent hydrogenation.

(v) The nitrogen content of the kerogen is not abnormal when compared with other kerogens and coals.

(vi) The need to concentrate the Tasmanite kerogen for most practical uses is clear. Physical methods are most appropriate and flotation will be discussed in the next report. Chemical methods, such as HCl/HF demineralization, are very effective but are, of course, impractical and highly expensive on a large scale.

(vii) No abnormal content of metals is organically bound within kerogen from Tasmanite.

4. BATCH AUTOCLAVE STUDY OF TASMANITE CONCENTRATE SAMPLE (77591) - CARBONIZATION IN NITROGEN AND UNCATALYSED AND CATALYSED HYDROGENATION:

I. Introduction

A programme of batch autoclave experiments was undertaken, using a subsample of tasmanite concentrate sample 77591, in order to study the carbonization, uncatalysed hydrogenation and catalysed hydrogenation of

liptinite (≡ exinite). The petrographic and chemical data for this tasmanite concentrate subsample (77591/3) are presented in Table 5. The preparation of the tasmanite concentrate sample is described elsewhere.

II. Experimental

II a. Autoclave Equipment

The batch autoclave experiments were carried out in an unstirred, 50 ml capacity, stainless steel (SUS 316) autoclave designed for high-pressure, single-cell, differential thermal analysis (DTA)[1,2] This autoclave equipment is illustrated in Figure 2. The autoclave was heated in a 76 mm diameter, vertical tube furnace; a constant heating rate of 3°C/minute was achieved by a series of manual settings of a voltage slider. At the completion of the experimental run, the autoclave was quenched by rapid withdrawal from the tube furnace, using a pulley system, and cooling by means of an electric fan.

II b. Batch Autoclave Experiments

The batch autoclave experiments were carried out using a nitrogen or a hydrogen atmosphere heating the tasmanite concentrate to eleven reaction temperatures between 200°C and 480°C. The temperatures between 370°C and 480°C were selected on the basis of the DTA curve characteristics of the experimental runs for tasmanite concentrate heated to 480°C. In addition to the uncatalysed experimental runs, batch autoclave experiments were carried out using tin(II) chloride and zinc(II) chloride as catalysts. The experimental conditions for the batch autoclave experiments are listed in Table 6.

During each autoclave experiment temperature, pressure, and the temperature difference (ΔT°C) between the sample and a reference material, were recorded. The reference material was a stainless steel cylinder located directly beneath the sample (see Figure 2a). The pressure was recorded by means of a pressure transducer; the pressure curve on the chart recorder was calibrated against a standard safety pressure gauge.

II c. Sampling and Analysis of Autoclave Gas Samples

At the end of each autoclave experiment the autoclave was cooled

to ambient temperature and the final pressure recorded. The autoclave was vented and a gas sample collected at 50 kg/cm^2 (4.90 MPa) in a 430 ml glass gas sample vessel. A second gas sample was collected at 20 kg/cm^2 (1.96 MPa) in a 150 ml glass gas sample vessel for twenty two of the experimental runs.

The gas samples were analysed on a Hewlett Packard 5830A gas chromatograph (GC) equipped with a Hewlett Packard 18850 GC terminal. The details of the GC analytical conditions are summarized in Table 7.

The GC equipment was calibrated using air and two standard hydrocarbon gas samples, namely a propane-isobutane-isobutene-normal butane mixture and a methane-ethane-ethylene-propylene mixture, to check the retention times and response factors.

II d. Sampling of the Liquid and Solid Autoclave Products

In order to avoid the physical disintegration of the solid residues, in particular the coherent plugs of carbonaceous material, the autoclave residues were cold extracted with normal hexane in the absence of any agitation. The cold hexane extraction was repeated until the residue ceased to yield a coloured solution on standing in normal hexane.

The hexane extract was separated from the solid residue by careful decantation and filtering. The hexane extract was then heated under a vacuum in a rotary evaporator to remove the normal hexane. Once the latter had been distilled off, the hexane extract was transferred to a weighed glass tube, by dissolving it in a minimum amount of dichloromethane (methylene chloride), and dried in a flow of nitrogen. Finally, the hexane extracts, together with the hexane insoluble residues, were placed overnight in a vacuum oven (500 nm of mercury) at 80°C. The weights of the hexane extract and the hexane insoluble residue were recorded.

Curie point pyrolysis gas chromatographic analyses were carried out on selected hexane extracts using a Pye Pyrolyser-Hewlett Packard 5710A gas chromatograph - Hewlett Packard 3385A Automation System. The analytical conditions are as follows:

011

146012

Wire temperature	610°C
Pyrolysis time	12,5 seconds
Carrier gas	Helium
Flow rate	4 ml/minute
Oven temperature	Ambient temperature 2 minutes
	50°C → 260°C at 4°C/minute
Chart speed	0.3 cm/minute

II e. Preparation of the Solid Residues for Petrographic Examination

A portion of each of the solid residues was set aside for the preparation of polished specimens for examination by incident light microscopy. The solid plugs were carefully cut in half, parallel to the axis of the autoclave, and the orientation of the half plug was noted. The porous plugs were vacuum impregnated with Araldite prior to embedding in Araldite in a cylindrical mould. The solid residue mounts were ground down under water on a series of wet and dry silicon carbide papers (240#, 400# and 600#). The residues were then polished with an aqueous slurry of green chrome oxide on Buehler Metcloth on a rotating lap and subsequently polished with an aqueous slurry of Magomet (magnesium oxide) on Selvyt cloth on a rotating lap. It proved necessary to vacuum impregnate some of the mounted residues with Araldite on completion of the grinding, since they were too porous and/or too friable for successful polishing to be achieved. After polishing with Magomet, each of the polished specimens was buffed on a clean, wet, strip of Selvyt cloth and blotted dry on a clean filter paper. Traces of polishing powder, that adhere to the surface of the polished specimen, were removed by immersion in an ultrasonic bath on completion of the chrome oxide and Magomet polishing stages.

II f. Petrographic Examination of the Solid Residues

An incident light, microscopic examination of the polished residues was carried out, using both air and oil immersion objectives, by means of a Zeiss Universal microscope. In the first instance the residues were examined in air, initially under incident, white light (100W/12V quartz halogen lamp) conditions and subsequently under incident, blue-light excitation (490 nm excitation filter, 500 nm dichroic reflector, 520 nm barrier filter and a 50W mercury lamp). In addition the residues were carefully examined under incident, ultraviolet-light excitation

012

(365 nm exciter filter, 400 nm dichroic reflector, 460 nm barrier filter and a 250W high-pressure mercury lamp) on a Leitz-Wetzlar Orthoplan-POL microscope.

The residues were then examined under oil immersion (Zeiss immersion oil 518C; n_D = 1.515, n_e = 1.518 at 23°C) using both white light and fluorescent light. Reflectivity measurements were carried out at 546 nm (n_e) using a Zeiss MPM 03 microscope photometer/digital read out system attached to the Zeiss Universal microscope. Both sapphire (n_e = 1.77) and yttrium aluminium garnet (YAG) (n_e = 1.84) reflectivity standards were used to calibrate the microscope photometer. The calculated R_o values for these reflectivity standards are 0.587% and 0.920%, respectively.

III. RESULTS

III a. Batch Autoclave Experimental Data

Table 8 sets out the batch autoclave experiment data. A few of the values for ΔT°C and pressure are regarded as being unreliable, due to autoclave leaks and/or failure to maintain a constant heating rate; these values are placed in parenthesis. The batch autoclave experiment data are illustrated in Figures 3 and 4. The curves for pressure against temperature, ΔT°C against temperature, and rate of pressure change against temperature (dP/dT) are based on the experimental runs carried out at 480°C. The individual data points listed in Table 8 are not plotted in Figures 3 and 4.

The batch autoclave experiment data for a nitrogen atmosphere indicate an increase in the value of dP/dT above 400°C and a sharp exothermic peak with a maximum at 425°C. By comparison, the batch autoclave experiments using a hydrogen atmosphere yield data that indicate one, or more, relatively broad exothermic peaks and a minimum dP/dT value that coincides with the principal exothermic peak:-

Experiment	Exothermic Peaks: Temperature of maximum value	Temperature of dP/dT minimum value
N_2	425°C	-
H_2	440°C	440°C
$H_2 + SnCl_2$	380°C, 425°C	390°C
$H_2 + ZnCl_2$	310°C, 425-450°C	430°C

III b. Composition of Autoclave Gas Samples

The final pressure values, listed in Table 8, are plotted against temperature in Figure 5. The compositions of the autoclave gas samples are presented in Tables 9 to 12, inclusive. Hydrocarbon gas ratios are presented in Table 13.

For the batch autoclave experiments carried out using a nitrogen atmosphere, Figure 5 shows that there is a steady increase in the final pressure with increase in the reaction temperature above 350°C. Reference to Tables 9 and 10 and Figure 6 indicates that this increase in the final pressure corresponds with a decrease in the proportion of nitrogen in the autoclave gas with increase in the reaction temperature.

For the batch autoclave experiments carried out using a hydrogen atmosphere, Figure 5 shows that there is a decrease in the final pressure with increase in the reaction temperature at higher temperatures. Tables 9 and 10 and Figure 6 indicate that there is a decrease in the proportion of hydrogen in the autoclave gas with increase in the reaction temperature above 300°C to 350°C.

Figures 7 and 8 illustrate the proportions of carbon monoxide, carbon dioxide and hydrocarbons present in the autoclave gas at reaction temperatures between 300°C and 480°C. The data for the uncatalysed batch autoclave experiments exhibit similar trends:

(i) A steady increase in the proportion of carbon dioxide with increase in temperature.

(ii) A rapid increase in the proportions of methane and C_3-C_6 hydrocarbons with increase in temperature above 425°C.

(iii) The formation of small quantities of ethane above 425°C.

Small quantities of carbon monoxide are formed at temperatures above 330°C; the uncatalysed hydrogenation experiments yield higher proportions of carbon monoxide than the corresponding batch autoclave experiments carried out using a nitrogen atmosphere.

The catalysed hydrogenation experiments exhibit different trends from those shown by the uncatalysed batch autoclave experiments. Reference to Tables 9 and 10 and Figures 7 and 8 indicate the following trends:

(i) A relatively small increase in the proportion of carbon dioxide with increase in temperature.

(ii) A rapid increase in the proportions of methane and C_3-C_6 hydrocarbons with increase in temperature above 425°C to 450°C.

(iii) The formation of appreciable quantities of ethane above 350°C; the proportion of ethane in the autoclave gas reaches a maximum at 450°C. Ethane is the principal hydrocarbon component formed between 350°C and 450°C.

(iv) The formation of very small quantities of ethylene at temperatures as low as 300°C; the proportion of ethylene in the autoclave gas reaches a maximum between 350°C and 370°C. Ethylene is the principal hydrocarbon component formed between 300°C and 350°C.

Figures 9 and 10 illustrate the relative proportions of carbon monoxide, carbon dioxide and hydrocarbons in the autoclave gas samples. These figures serve to emphasize the sympathetic relationship between ethane and the proportions of methane and C_1-C_6 hydrocarbons in the case of the uncatalysed autoclave experiments. This is in contrast to the antipathetic relationship between ethane and ethylene, and ethane and the proportions of methane and C_1-C_6 hydrocarbons, in the case of the catalysed hydrogenation experiments.

Carbon monoxide is formed during the catalysed hydrogenation experiments. For the hydrogenation experiments catalysed with tin(II) chloride the proportions of carbon monoxide are similar to those for the batch autoclave experiments carried out using a nitrogen atmosphere. For the hydrogenation experiments catalysed with zinc(II) chloride the proportions of carbon monoxide are higher than those for the tin(II) chloride catalysed experiments, but lower than the proportions of carbon monoxide formed during the uncatalysed hydrogenation experiments.

Apart from low concentrations of ethylene, traces of other alkenes have been identified in the gas chromatograms. Propylene has been identified tentatively in the zinc(II) catalysed hydrogenation experiments carried out at 425°C. Isobutene has been identified tentatively in the uncatalysed experiments carried out at 415°C.

C_6 + compounds are present at very low concentrations in the autoclave gas from the catalysed hydrogenation experiments carried out at temperatures of 350°C and above.

A comparison between Tables 9 and 10 and Tables 11 and 12 show that the autoclave gas samples collected at 50 kg/cm^2 and 20 kg/cm^2 yield similar results in respect of the autoclave gas composition. The autoclave gas samples collected at 20 kg/cm^2 yield slightly lower proportions of cylinder gas than those collected at 50 kg/cm^2 (see Tables 9 and 10 and Figure 6).

Reference to Tables 9 and 10 indicates that the $C_1/(C_1$ to $C_6)$ value decreases from close to unity at 390°C to 0.5-0.6 at 480°C for the uncatalysed batch autoclave experiments. Whereas the $C_1/(C_1$ to $C_6)$ value for the catalysed batch autoclave experiments increases from nearly zero at 390°C to about 0,5 at 480°C (see Figure 9). However, since, as has already been stated, ethane does not vary sympathetically with methane and the C_1-C_6 hydrocarbons for the catalysed hydrogenation experiments, it is of more interest to consider the hydrogenation ratios presented in Table 13 and illustrated in Figure 9, from which the following trends can be established:

(i) The value of $C_1/(C_1 + C_3$ to $C_6)$ exhibits a similar trend to that for $C_1/(C_1$ to $C_6)$. Apart from the values at 390°C, the $C_1/(C_1$ to $C_6)$ value is relatively constant ($\sim$ 0.6) for the uncatalysed batch autoclave experiments. The $C_1/(C_1$ to $C_6)$ value for the catalysed batch autoclave experiments increases with the reaction temperature from zero at 370°C to converge on a value of about 0,6 between 425°C and 450°C.

(ii) For the uncatalysed batch autoclave experiments the $C_1/(C_1 + C_2)$ value is close to unity, whereas that for the catalysed batch autoclave experiments increases from zero between 370°C and 390°C to approach unity at temperatures above 480°C.

(iii) Between 415°C and 450°C the $C_1/(C_1 + C_3)$ values for the uncatalysed and catalysed batch autoclave experiments approach a constant value of about 0.70.

(iv) Between 415°C and 425°C the $C_1/(C_1 + C_4)$ values for the uncatalysed and catalysed batch autoclave experiments approach a constant value of about 0.85.

(v) The low concentrations of pentane in the autoclave gas are reflected in $C_1/(C_1 + C_5)$ values close to unity.

(vi) Between 415°C and 425°C the $C_3/(C_3 + C_4)$ value approaches a constant value of about 0.7 for both the uncatalysed and catalysed batch autoclave experiments.

(vii) The $i\text{-}C_4/(i\text{-}C_4 + n\text{-}C_4)$ value for the uncatalysed batch autoclave experiments increases from about zero at 415°C to about 0.15 at 480°C. Whereas the $i\text{-}C_4/(i\text{-}C_4 + n\text{-}C_4)$ value for the catalysed batch autoclave experiments decreases from unity at 370°C to 0.3-0.4 at 480°C.

(viii) The $i\text{-}C_5/(i\text{-}C_5 + n\text{-}C_5)$ value for the uncatalysed batch autoclave experiments using a nitrogen atmosphere increases from zero at 425°C to about 0.2 at 480°C. Isopentane was not detected in the uncatalysed hydrogenation experiments. The $i\text{-}C_5/(i\text{-}C_5 + n\text{-}C_5)$ value for the catalysed hydrogenation experiments decreases from unity at 425°C to 0.5-0.6 at 480°C.

Although not detected by gas chromatographic analysis, hydrogen sulphide is present in the autoclave gas samples. It was detected by its characteristic odour in gas samples from the batch autoclave experiments run at temperatures in excess of 350°C. The odour of hydrogen sulphide was not detected in gas samples from the tin(II) chloride catalysed experiments run at high temperatures. The presence of hydrogen sulphide was confirmed for a number of the autoclave gas samples by passing the gas through a silver nitrate solution on completion of the gas analysis.

Nitrogen and oxygen are present in the autoclave gas samples collected from the hydrogenation experiments and oxygen is present in the autoclave gas samples collected from the nitrogen atmosphere experiments. These gases are derived from sorbed air present in the tasmanite concentrate. They constitute a very small proportion of the total gas sample and they have been disregarded in the presentation of the autoclave gas data.

III c. Liquid and Solid Autoclave Products

Table 14 presents data for the hexane insoluble material and the hexane extract (heavy (C_{10}+) hydrocarbons) obtained from the tasmanite concentrate for the various reaction temperatures. The percentage conversion data are calculated as follows:

(1) % conversion to (oil+gas+water) $= \left[100 \frac{5-(\text{wt. hexane insoluble residue+wt. catalyst})}{(5-\text{wt. catalyst})}\right]$

(2) % conversion to heavy(C_{10}+) hydrocarbons $= \left[100 \frac{(\text{wt. hexane extract})}{(5-\text{wt. catalyst})}\right]$

(3) % conversion to (light oil+gas+water) = (1)-(2)

(4) % hexane insoluble residue = 100-(1)

Ideally the conversion percentage should be expressed on a dry ash free (d.a.f.) basis; however, this would necessitate proximate analyses being carried out on the solid residues. Since the latter are required for the preparation of polished samples for microscopic examination and for other analyses, there was insufficient material available for proximate analysis.

For the nitrogen atmosphere experiments the maximum generation of heavy hydrocarbons occurs at 425°C. For the uncatalysed hydrogenation and the zinc(II) chloride catalysed hydrogenation experiments the maximum generation of heavy hydrocarbons occurs at 425°C and 450°C. For the tin(II) chloride catalysed hydrogenation experiments the maximum generation of heavy hydrocarbons occurs at 450°C.

Only small quantities (< 6%) of heavy hydrocarbons are generated at temperatures below 390°C. At temperatures above 425°C to 450°C the yield of heavy hydrocarbons decreases; less than 20% of heavy hydrocarbons are formed at 480°C.

There is a steady increase in the proportion of (light oil + gas + water) with increase in the reaction temperature; at 480°C the (light oil + gas + water) fraction constitutes 35% to 45% of the autoclave products.

The yields of heavy hydrocarbons at a given reaction temperature depend on the other experimental conditions. The maximum yields for the nitrogen atmosphere, uncatalysed hydrogenation and tin(II) chloride

catalysed hydrogenation experiments are 47.4%, 41.34% and 44.82%, respectively. The maximum yield of heavy hydrocarbons for the zinc(II) chloride catalysed hydrogenation experiments is less than that for the other experiments.

The Curie-point pyrolysis GC analyses yield chromatograms that reflect the differences in the experimental conditions at 415°C and 450°C.

(i) The nitrogen atmosphere experiment at 415°C yields a hexane extract containing C_{10} to C_{21} n-alkanes; there is also a C_{27} n-alkane peak. The C_{11} to C_{14} n-alkanes are the dominant constituents; they coincide with a lower molecular weight hump of unresolved branched and cyclic alkanes.

At 450°C the hexane extract contains C_{11} to C_{32} n-alkanes. The C_{12} to C_{16} n-alkanes are the dominant constituents; they coincide with a lower molecular weight hump of unresolved branched and cyclic alkanes.

(ii) The uncatalysed hydrogenation experiment at 415°C yields a hexane extract containing C_{11} to C_{31} n-alkanes. The C_{13} to C_{16} n-alkanes are the dominant constituents; they coincide with a lower molecular weight hump of unresolved branched and cyclic alkanes. There are significant amounts of a C_{15} isoprenoid alkane and a complex mixture of cyclic compounds(?) at higher carbon numbers.

At 450°C the hexane extract contains C_9 to C_{31} n-alkanes. The C_{10} to C_{14} n-alkanes are the dominant constituents; they coincide with a lower molecular weight hump of unresolved branched and cyclic alkanes. There is a second naphthenic hump in the C_{23} to C_{30} range. The C_{19} isoprenoid alkane, pristane, is present in the chromatogram.

(iii) The tin(II) chloride catalysed experiment at 415°C yields a hexane extract containing C_9 to C_{31} n-alkanes. The C_9 to C_{16} n-alkanes are the dominant constituents; they coincide with a lower molecular weight hump of unresolved branched and cyclic alkanes. There are small naphthenic humps between C_{17} and C_{20} and C_{26} and C_{29}. The C_{17} to C_{20} naphthenic hump contains a complex mixture of branched and/or cyclic alkanes.

The 450°C the hexane extract contains C_9 to C_{27} n-alkanes. The C_9 to C_{14} n-alkanes are the dominant constituents; the naphthenic hump occupies the C_{10} to C_{20} range.

019

(iv) The zinc(II) chloride catalysed experiment at 415°C yields a hexane extract containing C_{10} to C_{27} n-alkanes. The C_{12} to C_{17} n-alkanes are the dominant constituents; they coincide with a lower molecular weight hump of unresolved branched and cyclic hydrocarbons. The experiment at 450° yields similar results.

III d. Results of the Petrographic Examination of the Hexane-Insoluble Residues

Table 15 summarizes the changes in the macroscopic appearance of the hexane-insoluble residue with increase in the reaction temperature. In appearance the untreated tasmanite concentrate is a pale yellowish brown to medium brown powder. With increase in the reaction temperature the residue becomes progressively darker above 300°C to 350°C, forming a weakly-agglomerated to coherent, black residue between 390°C and 425°C.

The residue from the zinc(II) chloride catalysed hydrogenation reaction undergoes a change in appearance between 250°C and 300°C. Whereas the uncatalysed and tin(II) chloride catalysed hydrogenation reactions yield residues that do not exhibit any gross changes in appearance until a temperature of 350°C to 370°C has been reached.

The residue from the batch autoclave experiments using a nitrogen atmosphere forms a weakly agglomerated powder between 370°C and 390°C. The residue from the tin(II) chloride catalysed hydrogenation reaction does not form a coherent, black residue until a temperature of 415°C to 425° has been reached.

Microscopic examination of the residues permits variations in the optical behaviour of the alginite (Tasmanites sp bodies) to be related to the batch autoclave experimental conditions. Table 16 summarizes the changes in morphology, fluorescence behaviour and polishing relief of the alginite in response to increasing temperature.

The characteristic alginite morphology is unaffected by temperature increase between 200°C and 390°C, although there is a decrease in the polishing relief of the alginite between 350°C and 370°C in the case of the catalysed hydrogenation experiments. The development of very low polishing relief, and subsequent softening and flowing together, of the alginite occurs between 390°C and 425°C depending on the experimental

conditions. Above 425°C only small quantities of carbonaceous material remain to act as a matrix for the mineral matter and other inert constituents.

Untreated samples (30846 and 31773) of tasmanite concentrate yield a bright, very pale green to greenish yellow, alginite fluorescence under incident, ultraviolet-light excitation and a bright, canary yellow, alginite fluorescence under incident, blue-light excitation.

(a) The nitrogen atmosphere experiments represent the carbonization of alginite in an inert atmosphere and, as such, they can be regarded as analogous to the thermal maturation of alginite during burial metamorphism. The first change in the alginite fluorescence occurs between 250°C and 300°C, namely a reduction in fluorescence intensity. The change in colour from yellow to yellowish brown takes place between 350°C and 390°C. The alginite fluorescence disappears between 390°C and 415°C.

(b) The uncatalysed hydrogenation experiments exhibit alginite fluorescence changes with temperature that are similar to those exhibited by the nitrogen atmosphere experiments. However the reduction in fluorescence intensity does not take place until temperatures of 350°C to 370°C have been reached.

(c) The catalysed hydrogenation experiments yield different alginite fluorescence trends with increase in temperature.

In the case of the zinc(II) chloride catalysed experiments there is a decrease in the alginite fluorescence intensity between 250°C and 330°C. Between 330°C and 350°C the alginite fluorescence changes from yellow to dull yellowish brown. The fluorescence disappears between 415°C and 425°C. At 415°C incident, ultraviolet-light excitation produces a very weak brownish fluorescence, whereas there is no fluorescence visible under incident blue-light excitation conditions.

In the case of the tin(II) chloride catalysed experiments the alginite fluorescence intensity and colour do not exhibit any major changes until temperatures of 370°C to 390°C have been reached. There appears to be a slight reduction in the fluorescence intensity between 200°C and 250°C and a slight increase in the fluorescence intensity between 300°C and 330°C. Between 370°C and 390°C there is a reduction in fluorescence intensity and

a colour change from yellow to dull yellowish brown. A change from dull yellowish brown to very dull dark brown occurs between 415°C and 425°C.

The reflectivity of the traces of vitrinite in the tasmanite concentrate is 0.37%, which is equivalent to a subbituminous coal rank. The reflectivity of the alginite is very low, i.e. $\bar{R}_o$ average = 0.07%, which is similar to that of the Araldite mounting medium. This similarity in reflectivity makes observation of the unaltered alginite difficult both in air and under oil immersion.

Despite the decrease in the fluorescence intensity and the change in the fluorescence colours with increase in the reaction temperature, the alginite reflectivity remains very low. This correlates with the decrease in the polishing relief with increase in the reaction temperature.. A few high relief, high reflectivity, carbonized alginites were observed in the nitrogen atmosphere experiment run at 425°C.

In the tin(II) chloride catalysed hydrogenation experiments the first appearance of tin(II) sulphide occurs at 300°C. With increase in the reaction temperature there is an increase in the grain size and abundance of this catalyst derivative. At temperatures above 350°C the aggregates of acicular tin(II) sulphide crystals are typically intimately associated with the alginite. Many of the alginite bodies are coated by crystal aggregates of tin(II) sulphide. There is no evidence for the formation of zinc(II) sulphide during the zinc(II) chloride catalysed hydrogenation experiments.

Some aspects of the alginite petrography are illustrated in Plates 1-3, inclusive.

IV. Interpretation and Discussion of Results

IV a. Batch Autoclave Experimental Data

A glass sample tube (see Figure 2) was employed in the batch autoclave experiments in order to avoid possible memory effects due to transition metals (Fe, Ni, etc) in the stainless steel of the inner wall of the autoclave and the commonly used stainless steel sample vessel. Previous experience[3] using tin(II) chloride as a catalyst suggests that the catalyst reacts with the stainless steel of the sample vessel. A comparison between batch autoclave experiments employing a stainless steel sample tube and those employing a glass sample tube indicates that the use of the latter does not significantly influence the DTA data (unpublished work).

The interpretation of the DTA (ΔT°C) and differential pressure (dP/dT) data for the batch autoclave experiments is based on CSIRO Fuel Geoscience Unit experience[1,2,4].

(i) The batch autoclave experiments carried out using a nitrogen atmosphere represent the carbonization of the tasmanite concentrate in an inert atmosphere. The single exothermic peak in the DTA curve at 425°C is thought to represent a phase change, i.e. the formation of a fluid phase[5]. The increase in the dP/dT value above 400°C represents the formation of appreciable quantities of gaseous products.

(ii) The batch autoclave experiments carried out using a hydrogen atmosphere represent the uncatalysed hydrogenation of the tasmanite concentrate. The broad exothermic peak with a maximum value at 440°C corresponds with a minimum in the dP/dT curve. In this case the broad exothermic peak is ascribed to the hydrogenation reaction and the dP/dT minimum represents maximum consumption of hydrogen by the tasmanite concentrate. The effect of any phase change is masked by the hydrogenation reaction.

(iii) The batch autoclave experiments carried out using tin(II) chloride and zinc(II) chloride represent the catalysed hydrogenation of the tasmanite concentrate. The DTA and dP/dT data suggest that these catalysts influence the hydrogenation reaction in different ways.

(a) In the case of the tin(II) chloride catalysed hydrogenation experiments the principal exothermic peak has a maximum at 380°C. This maximum almost coincides with the dP/dT minimum at 390°C. Together they reflect the principal hydrogenation reaction. A satellite exothermic peak at 425°C is thought to represent the formation of a fluid phase.

(b) In the case of the zinc(II) chloride catalysed hydrogenation experiments there is a broad exothermic peak at 310°C and a slight exothermic rise between 360°C and 390°C. The broad exothermic peak in the 425°C to 450°C temperature range coincides with the dP/dT minimum at 430°C; together they represent the hydrogenation reaction. The effect of any phase change is masked by the hydrogenation reaction.

In view of the high ash content of the tasmanite concentrate, it was not thought necessary to employ an inert diluent, e.g. alumina, to prevent the formation of mesophase in the unstirred autoclave. The use of alumina to enhance hydrogen availability, by inhibiting agglomeration of carbonaceous material at temperatures above 400°C, has already been demonstrated for low-ash samples[2].

IV b. Autoclave Gas Composition

The batch autoclave experiments carried out using a nitrogen atmosphere yield final pressure values that reflect the volume of gas generated, since nitrogen is inert and plays no part in the thermal degradation of the tasmanite concentrate. For example, the experimental run to 480°C yields a final pressure of 105 kg/cm^2, i.e. a pressure increase of 5 kg/cm^2 which corresponds with the generation of 5% (by volume) of gas.

The hydrogenation experiments yield final pressure values that reflect the volume of gas generated less the volume of hydrogen consumed. At 480°C the hydrogenation experiments yield 4% to 6% (by volume) of gas. The uncatalysed and zinc(II) chloride catalysed hydrogenation experiments exhibit a small pressure loss, i.e. 2 kg/cm^2; whereas the tin(II) chloride catalysed experiment exhibits an appreciable pressure loss, i.e. 11 kg/cm^2. This indicates that there is a much higher hydrogen consumption during the tin(II) chloride catalysed reaction than during the other hydrogenation reactions.

The uncatalysed batch autoclave experiments exhibit similar gas compositional trends with increase in reaction temperature. These trends represent the thermal cracking of the tasmanite concentrate. The tin(II) chloride and zinc(II) chloride catalysed hydrogenation experiments exhibit similar gas compositional trends with increase in reaction temperature. These trends, which are quite different from those for the uncatalysed experiments, represent the catalytic hydrocracking of the tasmanite concentrate.

Experimental studies of the hydrocracking of low temperature coal tar suggest that the thermal cracking of the tar produces a predominance of C_1 and C_2 gases; whereas the catalytic hydrocracking of the same material produces a predominance of C_3 and C_4 gases. With increase in the reaction

temperature there is a decrease in the value of $(C_3 + C_4)/(C_1 + C_2)$, which reflects the importance of thermal cracking at higher temperatures[6]. There is not much value in considering the $(C_3 + C_4)/(C_1 + C_2)$ value for the tasmanite concentrate batch autoclave experiments, since ethane and ethylene do not vary sympathetically with the proportion of methane present in the autoclave gas sample. However the catalysed hydrogenation experiments exhibit a decrease in the $(C_3 + C_4)/C_1$ value with increase in the reaction temperature, indicating an increase in the degree of thermal cracking of the tasmanite concentrate at higher temperatures.

The degree of hydrocarbon isomerization, i.e. the ratio of isoalkanes to normal alkanes, is of interest, since isomerization is characteristic of catalytic cracking.[6-8] Reference to Table 13 indicates that the isomerization ratio $(i\text{-}C_x)/(i\text{-}C_x + nC_x)$ is close to zero for the uncatalysed batch autoclave experiments. The isomerization ratio for the catalysed batch autoclave experiments decreases from close to unity in the 370° to 415°C temperature range to values of 0.3 to 0.4 and 0.5 to 0.6 for $(i\text{-}C_4)/(i\text{-}C_4+n\text{-}C_4)$ and $(i\text{-}C_5)/(i\text{-}C_5+nC_5)$ respectively, at 480°C.

The differences between the values of $C_1/(C_1 + C_2)$, $C_1/(C_1 + C_3)$ and $C_1/(C_1 + C_4)$ for the uncatalysed and catalysed batch autoclave experiments and the convergence of these sets of values to a constant figure in the 415°C to 450°C temperature range is related to decrease in catalytic activity at higher temperatures.

IV c. Liquid and Solid Autoclave Products

Reference to Table 14 and Figure 12 indicates that similar quantities of hexane insoluble material and hexane extract are formed at a given reaction temperature irrespective of the other experimental conditions.

In view of the reaction temperatures, i.e. 415°C and 450°C, and conditions under which the batch autoclave experiments were performed, the pyrolysis-GC chromatograms reflect the carbonization and hydrogenation products that have been vapourized onto the GC column during the Curie-point pyrolysis and not breakdown products of the hexane extract itself.

The pyrolysis-GC data can be interpreted in the following manner:

(i) In the case of the uncatalysed batch autoclave experiments the n-alkanes and the unresolved, lower molecular weight hump in the hexane extract chromatograms are ascribed to the direct thermal cleavage of the various bonds in the Tasmanite concentrate.

(ii) In the case of the uncatalysed hydrogenation experiment at 450°C the naphthenic hump at C_{23}-C_{30} is thought to reflect increased hydrogenation and cleavage of kerogen fragments.

(iii) The hexane extract chromatograms for the catalysed hydrogenation experiments indicate that there is a reduction in the complexity of the products with increase in the reaction temperature. At 450°C the hexane extract from the tin(II) chloride catalysed hydrogenation experiment has a higher proportion of lower molecular weight alkanes than that from the zinc(II) chloride catalysed hydrogenation experiment.

(iv) At 415°C the zinc(II) chloride catalysed experiment hexane extract has a much less complex chromatogram than that for the tin(II) chloride catalysed experiment; the tin(II) chloride catalysed hydrogenation reaction yields a greater range of branched and cyclic alkanes.

The conversion values in Table 14 refer to air dried material. Given that the untreated tasmanite concentrate contains 3.2% of moisture and 32.3% ash, the maximum percentage conversion of tasmanite concentrate to heavy hydrocarbons (hexane extract) is estimated to be 50% to 70% on a dry-ash-free basis, depending on the experimental conditions. Similarly the maximum percentage conversion to (oil + gas + water) is close to 100%. The increase in hexane-insoluble material above 450°C reflects the formation of asphaltene and/or char (mesophase) at the expense of the heavy hydrocarbons. A proportion of the latter is converted to light oil and gas at temperatures above 450°C; the proportion of gas formed from liquid products is assumed to increase with increase in temperature.

IV d. Petrography of the Hexane-Insoluble Residues

The variations in the macroscopic appearance of the tasmanite concentrate with increase in the reaction temperature reflect the changes in the optical behaviour of the alginite as observed by incident-light microscopy.

The formation of the coherent black residue at 425°C in the case of the tin(II) chloride catalysed experiments, and 415°C in the case of the other experiments, coincides with the softening and flowing together of the alginite.

The alteration in the tasmanite concentrate colour from medium brown to dark brown coincides with the reduction in the alginite fluorescence intensity and the change in colour from yellow to dull yellowish brown.

In the case of the tin(II) chloride catalysed experiments there is evidence to suggest that the initial reduction in the alginite fluorescence with increase in temperature is followed by an increase in the fluorescence intensity with further increase in temperature, prior to the major changes in fluorescence intensity and colour between 370°C and 390°C. The increase in the fluorescence intensity of exinite (sporinite and resinite) in hydrogenated vitrinite by comparison with that of exinite in adjacent unhydrogenated (carbonized) vitrinite has already been reported for coal hydrogenated in the presence of tin(II) chloride at temperatures below 400°C.[3]

Quantitative, incident, ultraviolet-light excitation fluorescence data have been reported for exinites heated for one hour in a nitrogen atmosphere at atmospheric pressure at temperatures between 200°C and 450°C. The fluorescence spectral maximum increases in wavelength from 560 nm (green) for the untreated exinite to 680 nm (reddish brown) for exinite heated at 350°C.[9] The results of the present study are broadly consistent with the fluorescence behaviour reported for these thermally altered exinites. Similar sporinite fluorescence trends have been reported for increase in coal rank caused by burial metamorphism.[10]

IV e. Discussion

A previous study involving the low temperature (thermolytic) treatment of the Mersey River (Permian) Tasmanites sp. and oil shale indicated that there is little change in the morphology and colour of the organic matter, even when it is heated at 280°C for periods in excess of thirty minutes.[11] These observations are consistent with those reported in the present study for the low temperature (<300°C) batch autoclave experiments. The resistance of alginite to hydrogenation at temperatures below 400°C has already been reported.[12]

The bulk of the oil is produced during the first thermolysis (10 minutes at 280°C) of the Tasmanites sp; the most abundant constituents are the C_{10} to C_{16} n-alkanes.[11] The hexane extract of the nitrogen atmosphere experiment heated to 415°C consists essentially of C_{10} to C_{16} n-alkanes. Although there are differences between the thermolytic and batch autoclave experimental conditions, it appears that the hydrocarbon fraction formed at about 300°C is similar to that formed at 400°C.

The batch autoclave experiments carried out using a nitrogen atmosphere yield alginite fluorescence data similar to that reported for heat-treated[9] and coalified[10] sporinites. The DTA exothermic peak at 425°C coincides with the elimination of the alginite; the macroscopic appearance of the residue changes from a coherent, black, pitch-like material to a black, sooty powder. The maximum generation of heavy hydrocarbons occurs at 425°C. The disappearance of alginite fluorescence takes place between 390°C and 415°C; at the latter temperature the alginite softens and flows together.

The uncatalysed hydrogenation experiments yield similar results to those obtained for the nitrogen atmosphere experiments, except that the broad exothermic peak has a maximum at 440°C. The alginite softens and flows together at 415°C, but it still exhibits a weak fluorescence. The presence of hydrogen appears to slightly inhibit the loss of fluorescence. The maximum generation of oil occurs between 425°C and 450°C and it corresponds with the maximum hydrogen consumption reflected by the dP/dT minimum at 440°C and exothermic peak with a maximum at the same temperature.

The compositions of the autoclave gas samples indicate that the uncatalysed experiments are characterized by thermal breakdown reactions.

The catalysed batch autoclave experiments exhibit significant differences. The tin(II) chloride catalysed experiments are characterized by an exothermic peak maximum and a dP/dT minimum at 380°C to 390°C. However, at these temperatures the alginite is morphologically unchanged, apart from an increase in relief, and it still retains a relatively intense fluorescence. Thus the principal phase of hydrogenation results in little change in the optical behaviour of the alginite. The tin(II) sulphide, which is a catalyst derivative formed at temperatures above 300°C, is concentrated around the margins of the alginite. This suggests the breakdown of organic sulphur bonds in the alginite and scavenging of

the sulphur by tin. The presence of tin(II) sulphide in partially hydrogenated vitrinite has already been reported.[3]

The satellite DTA exothermic peak at 425°C coincides with the softening and flowing together of the alginite; even at this temperature the alginite displays a weak fluorescence. The maximum level of heavy hydrocarbon generation occurs at 450°C. It appears that in the case of the tin(II) chloride catalysed hydrogenation experiments the hydrogenation reaction precedes the melting of the alginite. The presence of tin(II) chloride appears to inhibit changes in the optical behaviour of the alginite with increase in the reaction temperature until the softening point at 425°C is reached.

The zinc(II) chloride catalysed experiments are characterized by an exothermic peak at 310°C which corresponds with a noticeable loss in alginite fluorescence intensity. There is only a slight exothermic rise between 360°C and 390°C. This is in marked contrast to the behaviour of vitrinite from a high-volatile bituminous coal, for which both tin(II) chloride and zinc(II) chloride produce DTA exothermic maxima and dP/dT minima at 360°C to 390°C [1,2] (unpublished work). The zinc(II) chloride catalysed hydrogenation reaction for alginite appears to proceed by a different mechanism from that catalysed by tin(II) chloride. The hydrogenation of high volatile, vitrinite-rich, bituminous coal with tin(IL) chloride yields similar DTA and dP/dT data to those reported for the tin(II) chloride catalysed hydrogenation experiments in this report (unpublished work). There are similarities between the optical behaviour of alginite described in this report and that of sporinite observed in partially hydrogenated vitrinite catalysed by tin(II) chloride.[3]

In the zinc(II) chloride catalysed hydrogenation experiments that alginite fluorescence becomes very weak between 350°C and 370°C, although the alginite does not soften until 415°C. The DTA and dP/dT data indicate that the maximum phase of hydrogenation does not take place until temperatures of 425°C to 450°C have been reached, which corresponds with the maximum level of heavy hydrocarbon generation.

The autoclave gas sample compositions indicate that the tin(II) chloride and zinc(II) chloride catalysed hydrogenation experiments are characterized by themocatalytic reactions at the lower reaction temperatures. At higher

reaction temperatures thermal breakdown reactions become more important in the gas forming process. The generation of ethylene at relatively low reaction temperatures (300°C-350°C) is of interest; at higher temperatures ethane appears to be formed at the expense of the ethylene. The decrease in the alginite fluorescence intensity between 250°C and 330°C, may be related to the generation of the ethylene. In the case of the tin(II) chloride catalysed hydrogenation experiments only small quantities of ethylene are formed; the alginite fluorescence intensity decrease ceases between 300°C and 330°C. In the case of the zinc(II) chloride catalysed hydrogenation experiments larger quantities of ethylene are formed; the alginite fluorescence intensity decreases steadily between 250°C and 370°C.

The absence of the characteristic odour of hydrogen sulphide in the autoclave gas samples from the tin(II) chloride catalysed hydrogenation experiments is due to the scavenging of sulphur by tin.

5. FLASH PYROLYSIS OF TASMANITE

Several shale samples were subjected to flash pyrolysis in the laboratory-scale apparatus developed by R. Tyler in the CSIRO Division of Process Technology. In this method a pulverized sample is heated rapidly (< 1 second) to the desired temperature and the resulting volatiles are cooled as quickly as possible to avoid secondary effects. Using a feed containing 59.4% mineral matter the yield of tar at 506°, 556° and 607°C was ∿ 25% and at 653°C the yield dropped off slightly. Under all conditions there was an almost complete conversion of organic carbon to volatile matter. Since the tasmanite kerogen is very rich in hydrogen, a similar yield is also obtained at slower heating rates and so no great advantage results from flash pyrolysis technique. Some microanalytical data on the tars is given in Table 17. The difference percentage, which represents mainly oxygen but with appreciable sulphur and some nitrogen, is lower than for most coals. Black coals under flash pyrolysis conditions commonly give 10-16%, while tars from brown coals often contain ∿ 18% oxygen + sulphur + nitrogen. Interestingly the atomic H/C of the tars decreases with increasing pyrolysis temperature and is always less than the H/C ratio of the initial kerogen. All the tars produced were quite mobile but would still require considerable treatment before a low-sulphur product suitable for a refinery or petrochemical plant could be obtained.

6. BIBLIOGRAPHY

1. Makino, K., Ueda, S. and Shibaoka, M. (1968). Application of a single-cell high-pressure DTA technique to coal hydrogenation research. Fuel, 57, 655-656.

2. Yokoyama, S., Ueda, S. Maekawa, Y., and Shibaoka, M. (1979). Studies on coal hydrogenation reaction using high pressure differential thermal analysis. Paper presented at ACS/CSJ Chemical Congress, Honolulu, Hawaii, April, 1979.

3. Shibaoka, M., Ueda, S., and Russell, N.J. (1979). Some aspects of the behaviour of tin(II) chloride during coal hydrogenation in the absence of a solvent. Submitted to Fuel, 1979.

4. Shibaoka, M. and Ueda, S. (1978). Formation and stability of mesophase during coal hydrogenation. 1. Formation of mesophase. Fuel, 57, 667-672.

5. Oberlin, A., Villey, M., and Combaz, A. (1978). Pyrolysis mechanism as studied by electron microscopy, DTA, IR and ESR. Carbon, 16, 73-74.

6. Qader, S.A. and Hill, G.R. (1969). Catalytic hydrocracking. Mechanism of hydrocracking of low temperature coal tar. Industrial and Engineering Chemistry Process Design and Development, 8, 456-461.

7. Qader, S.A. and Hill, G.R. (1969) Catalytic hydrocracking. Hydrocracking of a low temperature coal tar. Industrial and Engineering Chemistry Process Design and Development, 8, 450-455.

8. Qader, S.A. and Hill, G.R. (1969). Hydrocracking of petroleum and coal oils. Industrial and Engineering Chemistry Process Design and Development, 8, 462-469.

9. Ting, F.T.C. and Loo, H.B. (1975). Fluorescence characteristics of thermo-altered exinites (sporinites). Fuel, 54, 201-204.

10. Ottenjann, K., Teichmüller, M., and Wolf, M. (1975). Spectral fluorescence measurements of sporinites in reflected light and their applicability for coalification studies. In "Pétrographie de la matière organique des sediménts, relations avec la paléotemperature at le potential pétrolier (ed. B. Alpern) (C.N.R.S., Paris), 49-64.

11. Combaz, A. (1971). Thermal degradation of sporopollenin and genesis of hydrocarbons. In "Sporopollenin" (ed. J. Brooks, P.R. Grant, M. Muir, P. van Gijzel and G. Shaw), Academic Press, 621-653.

12. Spackman, W., Davis, A., and Mitchell, G.D. (1976). The fluorescence of liptinite macerals. Brigham Young University Geology Studies, 22, 59-75.

7. ACKNOWLEDGEMENTS

The contributions of A. Finlay, G. Hansen, K. Maxwell, N. Morgan, E. Murray and R. Tyler to the work described in this report are gratefully acknowledged. The cooperation of the Tasmanian Department of Mines and the support of Endeavour Resources Limited are also appreciated.

Table 1. Chemical Separation of Tasmanite Kerogen

Treatment	Flotation Concentrate		China Flat Shale	
	Weight (g)	Lab. No.	Weight (g)	Lab. No.
	80.6	77591	150.2	78694
	↓		↓	
HCl, HCl/HF	57.1	77591K	31.8	78694K
	1.000	77591K	1.000	78694K
	↓		↓	
HCl/HF	0.800		0.780	
	↓		↓	
HCl/HF	0.765	77591KK	0.729	78694KK

Table 2. Elemental Composition of Tasmanite Kerogen

	77591KK		78694KK	
	%, dry basis	%, dry, mineral-free basis	%, dry basis	%, dry, mineral-free basis
C	79.34	82.3	67.58	82.8
H	10.59	11.0	88.3	10.8
N	0.68	0.7	0.80	1.0
S	4.0	4.0	10.6	3.1
O	1.89†	2.0	1.89†	2.3
F	1.0	-	1.4	-
Cl	<0.5	-	<0.5	-
Ash	2.4	-	11.7	-
Fe	0.06	-	7.15	-

† by difference

Table 3. Atomic Emission Spectrographic Analysis of Tasmanite Kerogens

(as parts per million, unless stated otherwise)*

Elements†	77591KK		78694KK	
	In Sample	In Ash‡	In Sample	In Ash‡
Ag	n0.03	n4	0.6	5
As			20	150
B	30	5,000	150	1,000
Be	n0.2	n25	n0.8	n6
Bi			0.4(?)	3(?)
Cd			n1	n8
Co	n0.3	n40	1(?)	10(?)
Cr	7	1,000	40	300
Cu	3	500	25	200
Ga	0.7	100	4	30
Ge	n0.6	n80	⩽0.3	⩽0.2
La	8	1,000	10	100
Mn	n	n	100	800
Mo	0.2	25	5	40
Ni	0.4	250	20	150
Pb	5	800	20	150
Sb			n0.2	n10
Sn	3	500	1	8
Ti	>250	>4%	>1,000	>1%
Tl			2	15
V	0.8(?)	100(?)	4(?)	30(?)
W			1	10
Y	10	1500	25	200
Yb	0.07	100	3	25
Zn	5(?)	800(?)	20	150
Zr	40	6,000	200	1500

* - no lines seen

n(x) - no lines seen - value is less than our detectability (xppm)

† In the case of Al, Ca, Fe, Mg, Na, P and Si lines were present but no estimate could be made

‡ The ash yield from 77591KK was 0.67%, that from 78694KK was 12.72%

Table 4. Petrographic Analyses of Demineralized Tasmanite Samples

% by volume

Sample	Lab. No.	Tasmanites	Other Organic Material	Mica	Pyrite	Quartz	Total No. of counts
Demineralized kerogen concentrate	77591K	97	Tr	Tr	Tr	3	82
Demineralized Bore No. 13B, 70'8½", 70'8½"-75'10" (21.6-23.1 m)	78694K	83	Tr	Tr	14	3	119

Tr - trace

* with only 100 points counted, the error associated with this method can be up to ± 10%

Table 5. Petrographic and Chemical Data for the Tasmanite Concentrate Subsample 77591/3

(A) Petrographic Data

(1) Maceral Analysis:

Vitrinite	1%
*Alginite	84%
Resinite	trace
Fusinite	trace
Semifusinite	
Macrinite	
Interodetrinite	
Clay Minerals	10%
Carbonate	trace
Quartz	5%
Feldspar	trace
Pyrite	trace

* Tasmanites sp

(2) Vitrinite Reflectivity

$\bar{R}_o$ average (546 nm)	0.39±0.06%
Range of R_o average values	0.28-0.48%

(B) Chemical Data

(1) Proximate Analysis

Air-Dried Basis

Moisture	3.2%
Ash	32.3%
Volatile Matter	60.4%
Fixed Carbon	4.1%

Dry Ash Free (d.a.f.) Basis

Volatile Matter	93.6%
Fixed Carbon	6.4%
Fuel Ratio (Fixed Carbon/ Volatile Matter)	0.068

(2) Ultimate Analysis

Air-Dried Basis

Carbon (uncorrected for CO_2)	48.7%
Hydrogen	6.5%
Nitrogen	0.5%
Sulphur (organic)	1.9%
Oxygen (by difference)	6.9%

Table 5 continued

037

Dry Ash Free Basis

Carbon	75.5%
Hydrogen	10.1%
Nitrogen	0.8%
Sulphur (organic)	2.9%
Oxygen (by difference)	10.7%
Atomic H/C	1.61
Atomic O/C	0.16

(3) Forms of Sulphur

Total Sulphur	3.14%
Pyritic Sulphur	0.10%
Sulphate Sulphur	1.14%
Organic Sulphur (by difference)	1.90%

(4) Specific Energy

Specific Energy	37.11 MJ/kg

Table 6. Batch Autoclave Study - Experimental Conditions

Autoclave Type:	Stainless steel (SUS 316) equipped with DTA head (unstirred)
Autoclave Capacity:	50 ml
Sample Container:	Stainless steel cylinder with glass liner (100 mm length x 22 mm diameter o.d.)
Sample Weight:	5 gms Tasmanite concentrate for uncatalysed experiments. 4.5 gms Tasmanite concentrate + 0.5 gms catalyst for catalysed experiments (Tasmanite concentrate impregnated with catalyst by means of an ethanolic metal halide solution)
Initial Pressure:	100 kg/cm^2 (9.80 MPa)
Initial Temperature:	Ambient (23°C-25°C)
Heating Rate:	3°C/minute
Reaction Temperatures:	200°C, 250°C, 300°C, 330°C, 350°C, 370°C, 390°C, 415°C, 425°C, 450°C and 480°C
Reaction Time:	0 (autoclave quenched on reaching the reaction temperature)
Cooling Rate:	20°C/minute over initial 100°C drop in temperature

RIKADENKI DOT PRINTING CHART RECORDER (BP SERIES)

Chart Attenuation	10 mv
Chart Speed	12 cm/h
Temperature Attenuation	0.5
DTA Attenuation	0.1

KYOWA PRESSURE TRANSDUCER CONTROLLER (PCT-500KV)

Attenuation	$1/100$
Cut-off Frequency	100 Hz
Strain	300×10^{-6}
B.V.	2 v
Capacity	500 kg/cm^2 (46 MPa)

Table 7. Operating Conditions for the Gas Chromatographic Analysis

70°C ISOTHERMAL PROGRAMME: HELIUM CARRIER: TC DETECTOR

Temperature 1	70°C
Time 1	70
Rate	1.0
Temperature 2	80°C
Time 2	0.0
Injection Temperature	70°C
FID Temperature	70°C
TCD Temperature	100°C
Oven Maximum	100°C
Chart Speed	0.5 cm/minute
Attenuation	2^6 or 2^8

Valve Changes

Time (minutes)	Valve
0.1	1
0.1	3
1.0 or 1.2	2
5.0	-1
12.0	-2
12.0	-3
13.0	3
17.0	-3
24.0	Stop

TCD Signal	A
Slope Sensitivity	0.2
Area Rejected	<1%
Flow Rate A	30 ml/minute } (within the range 29-30 ml/minute)
Flot Rate B	30 ml/minute
Option	0

Reference Column: 20" U.C.W. - 982 silicone on 80/100 mesh chromosorb W-HP

Analytical Columns: (1) 5' 30% DC 200 silicone oil on 80/100 mesh chromosorb P-AW
(2) 6' porapak Q 80/100 mesh
(3) 10' molecular sieve 5A 60/80 mesh

All columns are $\frac{1}{8}$" O.D. stainless steel

VALVES SWITCHING PROGRAMME (VALVES SWITCHED BY 75 psi AIR)

Valves Switched	Operation	(1)	(2)	(3)	Peaks Detected
1	Inject	→	→	→ By pass	
2	Elute Light H/C	→	→ By pass	→ By pass	C_3-C_5
1-	Backflush:Elute Heavy H/C	→ By pass ←	→ By pass	→ By pass	C_6
2-,3-	Transfer light gases	→ By pass ←	→	→	
3	Trap O_2,N_2,CH_4 in column 3	→ By pass ←	→	→ By pass	CO_2,C_2H_4 and C_2H_6
3-	Complete Elution	→ By pass ←	→	→	O_2, N_2 $CH_4$and CO

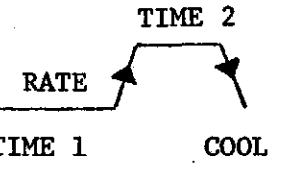

Table 8. Batch Autoclave Experiment Data

Experiment Number	Reaction Temperature (°C)	Catalyst	Cylinder Gas (Autoclave Atmosphere)	Differential Temperature (ΔT°C) at reaction temperature	Pressure at reaction temperature (kg/cm^2)	Final Pressure (kg/cm^2)
TC-26	200	-	N_2	-5.0	128	100
TC-25	200	-	H_2	-2.2	(123)	(95)
TC-37	200	$SnCl_2$	H_2	-4.9	(126)	(94)
TC-41	200	$ZnCl_2$	H_2	-3.5	128	100
TC-28	250	-	N_2	-7.3	139	100
TC-35	250	-	H_2	-3.1	132	100
TC-43	250	$SnCl_2$	H_2	-3.5	132	100
TC-42	250	$ZnCl_2$	H_2	-3.5	131	100
TC-32	300	-	N_2	-7.0	143	100
TC-24	300	-	H_2	-2.8	141	100
TC-22	300	$SnCl_2$	H_2	-2.0	141	100
TC-23	300	$ZnCl_2$	H_2	-2.9	139	100
TC-31	330	-	N_2	-5.8	(132)	(89)
TC-34	330	-	H_2	-3.5	142	100
TC-18	330	$SnCl_2$	H_2	-1.2	144	100
TC-21	330	$ZnCl_2$	H_2	-2.3	143	100
TC-27	350	-	N_2	-6.1	145	100
TC-33	350	-	H_2	-3.3	146	100
TC-16	350	$SnCl_2$	H_2	-0.9	146	99
TC-17	350	$ZnCl_2$	H_2	-3.3	146	100
TC-12	370	-	N_2	-5.9	153	101
TC-2	370	-	H_2	(-4.6)	151	100
TC-38	370	$SnCl_2$	H_2	-0.3	145	95
TC-40	370	$ZnCl_2$	H_2	-2.8	150	100
TC-11	390	-	N_2	-5.4	159	102
TC-5	390	-	H_2	-3.1	155	100
TC-36	390	$SnCl_2$	H_2	-0.3	144	92
TC-39	390	$ZnCl_2$	H_2	-0.5	152	100
TC-10	415	-	N_2	-6.1	161	102
TC-7	415	-	H_2	-3.6	154	100
TC-44	415	$SnCl_2$	H_2	-1.2	146	92
TC-45	415	$ZnCl_2$	H_2	-1.7	153	99
TC-8	425	-	N_2	-4.1	(161)	(102)
TC-4	425	-	H_2	-2.3	159	100
TC-48	425	$SnCl_2$	H_2	-1.2	147	91
TC-49	425	$ZnCl_2$	H_2	-2.0	155	98
TC-9	450	-	N_2	(-8.5)	(163)	(101)
TC-6	450	-	H_2	-1.8	159	99
TC-46	450	$SnCl_2$	H_2	-2.3	147	90
TC-47	450	$ZnCl_2$	H_2	-2.5	160	98
TC-1	480	-	N_2	-4.1	180	105
TC-3	480	-	H_2	-1.6	165	98
TC-13	480	$SnCl_2$	H_2	-2.8	151	89
TC-14	480	$ZnCl_2$	H_2	-1.8	162	98

Figures in parenthesis are regarded as less reliable.

(a) In the case of the ΔT°C values this is the result of failing to maintain a constant heating rate of 3°C/minute.

(b) In the case of the pressure values this is due to autoclave leakage, either from the copper seal or from one of the thermocouple entry ports in the autoclave head.

Table 9. Gas Chromatographic Analysis of Autoclave Gas Samples Collected at 50kg/cm^2 (Nitrogen+Oxygen free basis) (Volume %)

Experiment Number	Reaction Temperature (°C)	Catalyst	Cylinder Gas	Carbon Monoxide	Carbon Dioxide	Methane	Ethane	Propane	Butanes	Pentanes	C_6+ Compounds	Total Alkenes	Total Hydro-carbons	$\frac{C_1}{C_1-C_6}$	Cylinder Gas
TC-32	300	-	N_2	-	0.19	-	-	-	-	-	-	-	-	-	99.81
TC-24	300	-	H_2	-	0.19	-	-	-	-	-	-	-	-	-	99.81
TC-22	300	$SnCl_2$	H_2	tr	0.24			tr	-	-	-	[a]tr	tr	-	99.76
TC-23	300	$ZnCl_2$	H_2	-	0.29	-	-	-	-	-	-	0.06	0.06	-	99.65
TC-31	330	-	N_2	tr	0.24	tr	-	-	-	-	-	-	tr	-	99.76
TC-34	330	-	H_2	tr	0.24	tr	-	-	-	-	-	-	tr	-	99.76
TC-18	330	$SnCl_2$	H_2	tr	0.35	-	tr	0.01	-	-	-	[a]0.04	0.05	-	99.60
TC-21	330	$ZnCl_2$	H_2	tr	0.38	-	-	0.01	-	-	-	[a]0.09	0.10	-	99.52
TC-27	350	-	N_2	tr	0.30	tr	-	-	-	-	-	-	-	-	99.70
TC-33	350	-	H_2	tr	0.24	tr	-	0.01	-	-	-	-	0.01	-	99.75
TC-16	350	$SnCl_2$	H_2	tr	0.51	tr	tr	0.03	-	-	tr	[a]0.04	0.07	-	99.42
TC-17	350	$ZnCl_2$	H_2	tr	0.34	tr	-	0.04	0.01	-	tr	[a]0.08	0.13	-	99.53
TC-12	370	-	N_2	-	0.37	0.06	-	0.04	-	-	-	-	0.10	0.60	99.53
TC-2	370	-	H_2	0.02	0.35	0.06	-	0.04	-	-	-	-	0.10	0.60	99.53
TC-38	370	$SnCl_2$	H_2	tr	0.38	tr	0.20	0.07	tr	-	-	[a]tr	0.27	-	99.35
TC-40	370	$ZnCl_2$	H_2	0.02	0.44	tr	0.39	0.08	0.01	tr	-	[a]0.12	0.60	-	98.94
TC-11	390	-	N_2	-	0.47	0.13	-	0.02	-	-	-	-	0.16	0.87	99.38
TC-5	390	-	H_2	0.13	0.48	0.13	-	0.04	-	-	-	-	0.17	0.77	99.22
TC-36	390	$SnCl_2$	H_2	tr	0.38	tr	0.28	0.05	0.01	-	-	[a]tr	0.34	-	99.28
TC-39	390	$ZnCi_2$	H_2	0.12	0.49	0.06	0.30	0.15	0.03	tr	-	[a]tr	0.54	0.11	98.85
TC-10	415	-	N_2	0.02	0.79	0.32	-	0.15	0.01	tr	-	[b]0.01	0.49	0.67	98.67
TC-7	415	-	H_2	0.25	0.63	0.27	-	0.12	0.01	-	-	[b] tr	0.40	0.68	98.72
TC-44	415	$SnCl_2$	H_2	0.01	0.40	0.09	0.56	0.12	0.02	tr	-	[a] tr	0.79	0.11	98.80
TC-45	415	$ZnCl_2$	H_2	0.20	0.58	0.25	0.88	0.25	0.07	0.01	-	[a] tr	1.46	0.17	97.76
TC-8	425	-	N_2	0.08	0.89	0.42	-	0.18	0.08	0.01	-	-	0.69	0.61	98.34
TC-4	425	-	H_2	0.25	0.76	0.40	-	0.18	0.06	-	-	-	0.64	0.63	98.13
TC-48	425	$SnCl_2$	H_2	0.07	0.44	0.18	0.63	0.10	0.03	-	tr	[a]tr	0.94	0.19	98.55
TC-49	425	$ZnCl_2$	H_2	0.20	0.53	0.35	0.91	0.21	0.09	0.01	-	[c]0.04	1.57	0.22	97.67
TC-9	450	-	N_2	0.10	0.94	0.89	0.10	0.38	0.17	0.04	-	-	1.58	0.56	97.38
TC-6	450	-	H_2	0.33	0.99	1.00	0.12	0.40	0.15	0.02	-	-	1.66	0.60	97.02
TC-46	450	$SnCl_2$	H_2	0.08	0.47	0.42	0.86	0.22	0.08	tr	-	-	1.58	0.27	97.87
TC-47	450	$ZnCl_2$	H_2	0.19	0.53	0.91	1.13	0.37	0.12	0.01	tr	[a]tr	2.54	0.36	96.73
TC-1	480	-	N_2	0.09	1.14	2.07	0.36	0.99	0.40	0.11	tr	-	3.93	0.53	94.84
TC-3	480	-	H_2	0.36	0.99	2.02	0.05	1.02	0.30	0.01	-	-	3.40	0.59	95.25
TC-13	480	$SnCl_2$	H_2	0.13	0.54	1.73	0.31	0.87	0.33	0.05	tr	-	3.29	0.53	96.04
TC-14	480	$ZnCl_2$	H_2	0.22	0.55	1.73	0.78	0.64	0.28	0.09	tr	-	3.52	0.49	95.71

tr = trace a Ethylene b Iso-Butene? c Propylene?

$C_1/(C_1-C_6)$ = Methane/(C_1-C_6 alkanes)

042

146043

Table 10: Gas Chromatographic Analysis of Autoclave Gas Samples collected at 20kg/cm^2 (Nitrogen+Oxygen free basis) (Volume %)

Experiment Number	Reaction Temperature (°C)	Catalyst	Cylinder Gas	Carbon Monoxide	Carbon Dioxide	Methane	Ethane	Propane	Butanes	Pentanes	C_6+ Compounds	Total Alkenes	Total Hydro-carbons	$\frac{C_1}{C_1-C_6}$	Cylinder Gas
TC-32	300	-	N_2	-	0.21	-	-	-	-	-	-	-		-	99.79
TC-24	300	-	H_2	-	0.25	-	-	-	-	-	-	-	-	-	99.75
TC-22	300	$SnCl_2$	H_2	tr	0.31	-	-	-	-	-	-	[a]tr	tr	-	99.69
TC-23	300	$ZnCl_2$	H_2	tr	0.33	-	-	-	-	-	-	[a]0.07	0.07	-	99.60
TC-31	330	-	N_2	tr	0.29	tr	-	-	-	-	-	-	tr	-	99.71
TC-34	330	-	H_2	← not analysed →											
TC-18	330	$SnCl_2$	H_2	tr	0.39	-	-	0.01	-	-	-	[a]0.04	0.05	-	99.56
TC-21	330	$ZnCl_2$	H_2	tr	0.41	-	-	0.01	tr	-	-	[a]0.09	0.10	-	99.49
TC-27	350	-	N_2	tr	0.36	tr	-	-	-	-	-	-	-	-	99.64
TC-33	350	-	H_2	tr	0.33	tr	-	-	-	-	-	-	-	-	99.67
TC-16	350	$SnCl_2$	H_2	tr	0.42	tr	-	0.04	tr	-	tr	[a]0.05	0.09	-	99.49
TC-17	350	$ZnCl_2$	H_2	tr	0.35	-	-	0.04	0.01	-	tr	[a]0.08	0.13	-	99.52
TC-38	370	$SnCl_2$	H_2	tr	0.41	tr	0.23	0.04	tr	-	-	[a]tr	0.27	-	99.32
TC-40	370	$ZnCl_2$	H_2	0.06	0.51	tr	0.46	0.06	0.03	tr	tr	[a]0.14	0.55	-	98.74
TC-36	390	$SnCl_2$	H_2	tr	0.43	tr	0.32	0.07	0.02	tr	-	[a]tr	0.41	-	99.16
TC-39	390	$ZnCl_2$	H_2	0.13	0.52	0.07	0.32	0.18	0.04	tr	tr	[a]tr	0.61	0.12	98.74
TC-44	415	$SnCl_2$	H_2	0.07	0.47	0.12	0.71	0.13	0.03	tr	tr	[a]tr	0.99	0.12	98.46
TC-45	415	$ZnCl_2$	H_2	0.21	0.60	0.26	0.94	0.25	0.10	0.03	tr	[a]tr	1.58	0.17	97.61
TC-48	425	$SnCl_2$	H_2	0.07	0.50	0.20	0.72	0.13	0.05	tr	0.11	[a]tr	1.21	0.17	98.22
TC-49	425	$ZnCl_2$	H_2	0.21	0.58	0.38	0.99	0.25	0.12	0.05	tr	[a]tr	1.79	0.21	97.42
TC-46	450	$SnCl_2$	H_2	0.09	0.50	0.45	0.93	0.27	0.10	0.04	tr	-	1.79	0.25	97.62
TC-47	450	$ZnCl_2$	H_2	0.21	0.60	1.04	1.34	0.47	0.19	0.06	0.10	[a]tr	3.20	0.33	95.99
TC-13	480	$SnCl_2$	H_2	← not analysed →											
TC-14	480	$ZnCl_2$	H_2	0.26	0.63	2.53	0.92	0.93	0.42	0.13	tr	-	4.93	0.51	94.18

tr = trace a Ethylene

043

Table 11. Proportions of Carbon Monoxide, Carbon Dioxide and Hydrocarbons by volume in Autoclave Gas sample collected at 50kg/cm^2

Experiment Number	Reaction Temperature (°C)	Catalyst	Cylinder Gas	Carbon Monoxide	Carbon Dioxide	Methane	Ethane	Propane	Iso-Butane	Normal Butane	Iso-Pentane	Normal Pentane	C_6^+ Compounds	Total Alkanes	Total Alkenes
TC-32	300	-	N_2	-	100	-	-	-	-	-	-	-	-	-	-
TC-24	300	-	H_2	-	100	-	-	-	-	-	-	-	-	-	-
TC-22	300	$SnCl_2$	H_2	tr	100	-	-	tr		-	-	-	-	tr	[a]tr
TC-23	300	$ZnCl_2$	H_2	-	82.8	-	-	-	-	-	-	-	-	-	[a]17.2
TC-31	330	-	N_2	tr	100	tr	-	-	-	-	-	-	-	tr	-
TC-34	330	-	H_2	tr	100	tr	-	-	-	-	-	-	-	tr	-
TC-18	330	$SnCl_2$	H_2	tr	89.2	-	tr	1.6	-	-	-	-	-	1.6	[a]9.2
TC-21	330	$ZnCl_2$	H_2	tr	79.4	-	-	1.4	tr	-	-	-	-	1.4	[a]19.2
TC-27	350	-	N_2	tr	100	tr	-	-	-	-	-	-	-	-	-
TC-33	350	-	H_2	tr	94.7	tr	-	5.3	-	-	-	-	-	5.3	-
TC-16	350	$SnCl_2$	H_2	tr	88.0	tr	tr	5.0	-	-	-	-	tr	5.0	[a]7.0
TC-17	350	$ZnCl_2$	H_2	tr	74.6	tr	tr	7.7	1.6	-	-	-	tr	9.3	[a]16.1
TC-12	370	-	N_2	-	79.9	12.1	-	7.9	-	-	-	-	-	20.0	-
TC-2	370	-	H_2	4.5	75.6	12.0	-	7.9	-	-	-	-	-	19.9	-
TC-38	370	$SnCl_2$	H_2	tr	58.2	tr	31.1	10.7	tr	-	-	-	-	41.8	[a]tr
TC-40	370	$ZnCl_2$	H_2	1.6	41.2	tr	36.9	7.5	1.3	tr	tr	-	-	45.7	[a]11.5
TC-11	390	-	N_2	-	76.3	20.8	-	2.9	-	-	-	-	-	23.7	-
TC-5	390	-	H_2	16.3	62.1	16.3	-	5.3	-	-	-	-	-	21.6	-
TC-36	390	$SnCl_2$	H_2	tr	53.2	tr	38.8	6.9	0.7	0.4	-	-	-	46.8	[a]tr
TC-39	390	$ZnCl_2$	H_2	10.4	42.6	5.5	25.8	13.0	1.6	1.1	tr	-	-	47.0	[a]tr
TC-10	415	-	N_2	1.6	59.7	24.0	-	11.2	0.4	2.3	-	0.2	-	38.1	[b]0.6
TC-7	415	-	H_2	19.3	49.3	21.2	-	9.0	-	0.9	-	-	-	31.1	[b]0.3
TC-44	415	$SnCl_2$	H_2	0.9	33.2	7.3	46.9	10.4	0.6	0.7	tr	-	-	65.9	[a]tr
TC-45	415	$ZnCl_2$	H_2	8.9	25.8	11.2	39.1	11.1	1.8	1.5	0.6	tr	-	65.3	[a]tr
TC-8	425	-	N_2	4.6	53.4	25.3	-	11.0	0.5	4.4	-	0.8	-	42.0	-
TC-4	425	-	H_2	15.1	45.8	24.4	-	11.1	0.6	3.0	-	-	-	39.1	-
TC-48	425	$SnCl_2$	H_2	4.7	30.6	12.4	43.2	7.1	0.9	1.1	-	-	tr	64.7	[a]tr
TC-49	425	$ZnCl_2$	H_2	8.1	22.9	14.8	38.9	9.1	2.0	1.9	0.6	tr	-	69.0	[c]1.7
TC-9	450	-	N_2	3.8	35.9	34.0	3.8	14.7	0.7	5.5	0.1	1.5	0	60.3	-
TC-6	450	-	H_2	11.0	33.3	32.5	3.9	13.5	0.8	4.2	-	0.8	-	55.7	-
TC-46	450	$SnCl_2$	H_2	3.7	22.2	19.7	40.3	10.4	1.5	2.2	tr	tr	-	74.1	-
TC-47	450	$ZnCl_2$	H_2	5.7	16.5	27.9	34.6	11.3	1.8	1.9	0.3	tr	tr	77.8	[a]tr
TC-1	480	-	N_2	1.7	22.1	40.3	7.0	19.1	0.9	6.8	0.4	1.7	tr	76.2	-
TC-3	480	-	H_2	7.6	20.9	42.5	1.1	21.5	1.0	5.2	-	0.2	-	71.5	-
TC-13	480	$SnCl_2$	H_2	3.4	13.7	43.7	8.0	22.0	2.7	5.5	0.6	0.4	-	82.9	-
TC-14	480	$ZnCl_2$	H_2	5.2	12.7	40.4	18.2	14.9	2.5	4.0	1.1	1.0	tr	82.1	-

tr = trace a Ethylene b Iso-Butene? C Propylene?

044

Table 12. Proportions of Carbon Monoxide, Carbon Dioxide and Hydrocarbons by volume in Autoclave Gas Samples collected at 20kg/cm^2

Experiment Number	Reaction Temperature (°C)	Catalyst	Cylinder Gas	Carbon Monoxide	Carbon Dioxide	Methane	Ethane	Propane	Iso-Butane	Normal Butane	Iso-Pentane	Normal Pentane	C_6+ Compounds	Total Alkanes	Total Alkenes
TC-32	300	-	N_2	-	100.0	-	-	-	-	-	-	-	-	-	-
TC-24	300	-	H_2	-	100.0	-	-	-	-	-	-	-	-	-	-
TC-22	300	$SnCl_2$	H_2	tr	100.0	-	-	-	-	-	-	-	-	-	[a]tr
TC-23	300	$ZnCl_2$	H_2	tr	82.9	-	-	-	-	-	-	-	-	-	[a]17.1
TC-31	330	-	N_2	tr	100.0	tr	-	-	-	-	-	-	-	tr	-
TC-34	330	-	H_2	← not analysed →											
TC-18	330	$SnCl_2$	H_2	tr	88.7	-	-	2.0	-	-	-	-	-	-	[a]9.3
TC-21	330	$ZnCl_2$	H_2	tr	79.8	-	-	1.8	tr	-	-	-	-	1.8	[a]18.4
TC-27	350	-	N_2	tr	100.0	tr	-	-	-	-	-	-	-	tr	-
TC-33	350	-	H_2	tr	100.0	tr	-	-	-	-	-	-	-	tr	-
TC-16	350	$SnCl_2$	H_2	tr	82.4	tr	-	8.0	tr	-	-	-	tr	8.0	[a]9.6
TC-17	350	$ZnCl_2$	H_2	tr	74.0	-	-	8.1	1.8	tr	-	-	tr	9.9	[a]16.1
TC-38	370	$SnCl_2$	H_2	tr	59.6	tr	33.6	6.2	0.6	tr	-	-	-	40.4	[a]tr
TC-40	370	$ZnCl_2$	H_2	4.7	40.3	tr	36.8	5.1	1.8	0.4	tr	-	tr	44.1	[a]10.9
TC-36	390	$SnCl_2$	H_2	tr	51.1	tr	38.6	8.4	1.0	0.9	tr	-	-	48.9	[a]tr
TC-39	390	$ZnCl_2$	H_2	10.0	41.4	5.7	25.5	13.9	1.9	1.3	0.3	tr	tr	48.6	[a]tr
TC-44	415	$SnCl_2$	H_2	4.7	30.6	8.1	46.1	8.6	0.9	1.0	tr	tr	tr	64.7	[a]tr
TC-45	415	$ZnCl_2$	H_2	8.7	25.3	11.0	39.2	10.6	2.1	2.0	1.1	tr	tr	66.0	[a]tr
TC-48	425	$SnCl_2$	H_2	4.1	28.1	11.1	40.6	7.2	1.1	1.6	tr	tr	6.2	67.8	[a]tr
TC-49	425	$ZnCl_2$	H_2	8.0	22.4	14.6	38.5	9.8	2.3	2.4	1.3	0.7	tr	69.6	[ab]tr
TC-46	450	$SnCl_2$	H_2	3.6	21.1	18.8	39.2	11.2	1.7	2.7	1.0	0.7	tr	75.3	-
TC-47	450	$ZnCl_2$	H_2	5.3	15.0	26.1	33.3	11.7	2.2	2.5	0.9	0.5	2.5	79.7	[a]tr
TC-13	480	$SnCl_2$	H_2	← not analysed →											
TC-14	480	$ZnCl_2$	H_2	4.4	10.8	43.5	16.0	15.8	2.9	4.3	1.2	1.1	tr	84.8	-

tr = trace a Ethylene b Propylene?

Table 13. *Hydrocarbon Gas Ratios in Autoclave Gas Samples*

Experiment Number	$\frac{C_1}{C_1 + C_2}$		$\frac{C_1}{C_1 + C_3}$		$\frac{C_1}{C_1 + C_4}$		$\frac{C_1}{C_1 + C_5}$		$\frac{C_1}{C_1 + C_3 \text{ to } C_6}$		$\frac{C_3}{C_3 + C_4}$		$\frac{i\text{-}C_4}{i\text{-}C_4 + n\text{-}C_4}$		$\frac{i\text{-}C_5}{i\text{-}C_5 + n\text{-}C_5}$	
	50kg/cm^2	20kg/cm^2	50kg/cm^2	20kg/cm^2	50kg/cm^2	20kg/cm^2	50kg/cm^2	20kg/cm^2	50kg/cm^2	20kg/cm^2	50kg/cm^2	20kg/cm^2	50kg/cm^2	20kg/cm^2	50kg/cm^2	20kg/cm^2
TC-12	1.00	-	0.61	-	1.00	-	1.00	-	0.61	-	1.00	-	-	-	-	-
TC-2	1.00	-	0.60	-	1.00	-	1.00	-	0.60	-	1.00	-	-	-	-	-
TC-38	∿0.0		∿0.0	-	-	-	-	-	∿0.0	-	1.0	-	1.00	-	-	-
TC-40	∿0.0		∿0.0	-	∿0.0	-	-	-	∿0.0	-	0.85	-	1.0	-	1.00	-
TC-11	1.0	-	0.88	-	1.00	-	1.00	-	0.88	-	1.00	-	-	-	-	-
TC-5	1.0	-	0.76	-	1.00	-	1.00	-	0.76	-	1.00	-	-	-	-	-
TC-36	∿0.0		∿0.0	-	∿0.0	-	∿1.0	∿1.0	∿0.0	-	0.86	-	0.64	-	-	-
TC-39	0.18		0.30	-	0.67	-	∿1.0	-	0.26	-	0.83	-	0.59	-	1.00	-
TC-10	1.00	-	0.68	-	0.90	-	0.99	-	0.63	-	0.81	-	0.15	-	0.00	-
TC-7	1.00	-	0.70	-	0.96	-	1.00	-	0.68	-	0.91	-	0.00	-	-	-
TC-44	0.14	-	0.41	-	0.85	-	∿1.0	∿1.0	0.38	-	0.89	-	0.46	-	1.00	-
TC-45	0.22	-	0.50	-	0.77	-	0.95	-	0.43	-	0.77	-	0.55	-	1.0	-
TC-8	1.00	-	0.70	-	0.84	-	0.97	-	0.60	-	0.69	-	1.10	-	0.00	-
TC-4	1.00	-	0.69	-	0.87	-	1.00	-	0.62	-	0.76	-	0.17	-	-	-
TC-48	0.22	0.22	0.64	0.60	0.86	0.81	1.00	∿1.0	0.58	0.41	0.78	0.73	0.45	0.41	-	-
TC-49	0.28	0.22	0.62	0.60	0.79	0.76	0.96	0.88	0.52	0.47	0.70	0.68	0.51	0.49	1.0	0.65
TC-9	0.90	-	0.70	-	0.85	-	0.96	-	0.60	-	0.70	-	0.11	-	0.06	-
TC-6	0.88	-	0.71	-	0.87	-	0.98	-	0.63	-	0.73	-	0.16	-	0.00	-
TC-46	0.33	0.32	0.65	0.63	0.84	0.81	∿1.0	0.92	0.58	0.52	0.74	0.72	0.41	0.39	-	0.59
TC-47	0.45	0.44	0.71	0.69	0.88	0.85	0.99	0.95	0.65	0.56	0.75	0.71	0.49	0.47	1.00	0.64
TC-1	0.85	-	0.68	-	0.84	-	0.95	-	0.58	-	0.71	-	0.12	-	0.19	-
TC-3	0.98	-	0.66	-	0.87	-	1.00	-	0.60	-	0.78	-	0.16	-	0.00	-
TC-13	0.85	-	0.67	-	0.84	-	0.98	-	0.58	-	0.73	-	0.33	-	0.60	-
TC-14	0.69	0.73	0.73	0.73	0.86	0.86	0.95	0.95	0.63	0.63	0.70	0.69	0.39	0.40	0.52	0.52

046

Table 14. Liquid and Solid Autoclave Products

Reaction Temperature (°C)	Catalyst	Autoclave Atmosphere	Weight of Hexane-Insoluble Fraction (gms)	Weight of Hexane-Extract (gms)	Weight of Hexane Soluble Fraction (Weight Lost) (gms)	% (Light Oil + Gas + Water)	% Heavy (C_{10}+) Hydrocarbons	% Hexane Insoluble Material
200	-	N_2	4.760	0.039	0.240	4.02	0.78	95.20
	-	H_2	4.809	0.035	0.191	3.12	0.70	96.18
	$SnCl_2$	H_2	4.836	0.020	0.164	3.20	0.44	96.36
	$ZnCl_2$	H_2	4.923	0.015	0.077	1.38	0.33	98.29
250	-	N_2	4.676	0.053	0.324	5.42	1.06	93.52
	-	H_2	4.783	0.037	0.217	3.60	0.74	95.66
	$SnCl_2$	H_2	4.729	0.039	0.271	5.15	0.87	93.98
	$ZnCl_2$	H_2	4.933	0.010	0.067	1.27	0.22	98.51
300	-	N_2	4.667	0.049	0.333	5.68	0.98	93.34
	-	H_2	4.710	0.045	0.290	4.90	0.90	94.20
	$SnCl_2$	H_2	4.615	0.073	0.385	6.94	1.62	91.44
	$ZnCl_2$	H_2	4.696	0.057	0.304	5.49	1.27	93.24
330	-	N_2	4.570	0.058	0.430	7.44	1.16	91.40
	-	H_2	4.293	0.058	0.727	(12.98)	(1.16)	(85.86)
	$SnCl_2$	H_2	4.575	0.089	0.425	7.46	1.98	90.55
	$ZnCl_2$	H_2	4.471	0.131	0.529	8.85	2.91	88.24
350	-	N_2	4.442	0.093	0.558	9.30	1.86	88.84
	-	H_2	4.584	0.080	0.416	6.72	1.60	91.68
	$SnCl_2$	H_2	4.509	0.167	0.491	7.20	3.71	89.09
	$ZnCl_2$	H_2	4.326	0.214	0.674	10.22	4.76	85.02
370	-	N_2	4.248	0.187	0.752	11.30	3.74	84.96
	-	H_2	4.363	0.198	0.637	8.78	3.96	87.26
	$SnCl_2$	H_2	4.639	0.231	0.361	(2.89)	(5.13)	(91.98)
	$ZnCl_2$	H_2	4.106	0.255	0.894	14.20	5.67	80.13
390	-	N_2	3.966	0.412	1.034	12.44	8.24	79.32
	-	H_2	4.166	0.334	0.834	10.00	6.68	83.32
	$SnCl_2$	H_2	4.178	0.151	0.822	14.91	3.36	81.73
	$ZnCl_2$	H_2	3.827	0.538	1.173	14.07	12.00	73.93
415	-	N_2	2.676	1.237	2.324	21.74	24.74	53.52
	-	H_2	3.396	0.810	1.604	15.88	16.20	67.92
	$SnCl_2$	H_2	3.645	0.754	1.355	13.35	16.76	69.89
	$ZnCl_2$	H_2	3.053	1.040	1.947	20.16	23.11	56.73
425	-	N_2	1.548	2.370	3.452	21.64	47.40	30.96
	-	H_2	1.722	2.067	3.278	24.22	41.34	34.44
	$SnCl_2$	H_2	3.154	1.254	1.846	13.15	27.87	58.98
	$ZnCl_2$	H_2	2.199	1.374	2.801	31.71	30.53	37.76
450	-	N_2	2.025	1.338	2.975	32.74	26.76	40.50
	-	H_2	1.616	1.856	3.384	30.56	37.12	32.32
	$SnCl_2$	H_2	1.946	2.017	3.054	23.05	44.82	32.13
	$ZnCl_2$	H_2	2.353	1.307	2.647	29.78	29.04	41.18
480	-	N_2	2.424	0.535	2.576	40.82	10.70	48.48
	-	H_2	1.820	0.881	3.180	45.98	17.62	36.40
	$SnCl_2$	H_2	2.105	0.792	2.895	46.73	17.60	35.67
	$ZnCl_2$	H_2	2.378	0.882	2.622	38.67	19.60	41.73

Table 15. Macroscopic Appearance of Hexane-Insoluble Residue

Reaction Temperature (°C)	Nitrogen	Hydrogen	Hydrogen + Tin(II) Chloride	Hydrogen · Zinc(II) Chloride
200	Medium Brown Powder	Medium Brown Powder	Medium Brown Powder	Medium Brown Powder
250				
300				Medium to Dark Brown Powder
330	Medium to Dark Brown Powder			Dark Brown Powder
350				Dark Brown to Powder
370	Dark Brown to Blackish brown Powder	Medium to Dark Brown Powder	Medium to Dark Brown Powder	Dark Grey to Greyish Black Powder
390	Black Powder (Weakly agglomerated residue)	Dark Brown to Powder		
415	Coherent, pitch-like black residue	Black Powder (Very Weakly Agglomerated residue)	Dark Greyish Brown Powder	Coherent Dark Brown to Black Residue
425	Black Powder	Black Powder	Coherent Black Residue	Black Powder (Very Weakly Agglomerated Residue)
450	Black, Sooty Powder		Dark Grey to Greyish Black Powder	
480			Black Powder	Coherent Black Residue

The untreated Tasmanite concentrate is a pale yellowish brown to medium brown powder

Table 16: Microscopic appearance of Alginite in the Hexane-Insoluble Residues

Reaction Temperature (°C)		480	450	425	415	390	370	350	330	300	250	200
Nitrogen	Morphology	Mineral matter and inert constituents bound together by low relief matrix Some carbonized (high relief) and low-relief alginite at 425°C.			Alginite softens & flows together to form low relief material	Unaltered Alginite-moderately low relief	Alginite Morphology unaltered - low relief					
	U.V. Light	Matrix material exhibits a very weak brownish fluorescence (?)		No fluorescence		Dull yellowish brown fluorescence	Dull yellow to yellowish brown fluorescence	Bright greenish yellow to yellow fluorescence			Bright pale green to greenish yellow fluorescence	
	Blue Light	Yellowish fluorescence in araldite due to reaction with residue		No fluorescence		Dull yellowish brown to dull brown fluorescence	Dull yellow to yellowish brown fluorescence	Pale yellow fluorescence (+decrease in fluorescence intensity)			Bright yellow fluorescence	
Hydrogen	Morphology	Mineral matter and inert		Low relief material- a few	Very low relief alginite starting to soften & flow together	Alginite Morphology unaltered - low relief						
	U.V. Light	Very weak brownish fluorescence of matrix material-araldite fluorescence due to reaction with residue		No fluorescence	Very weak dark brown fluorescence	Dull yellow to yellowish brown fluorescence		Greenish yellow to yellowish brown fluorescence	Bright greenish yellow to yellow fluorescence		Bright pale green to greenish yellow fluorescence	
	Blue Light	Yellowish fluorescence in araldite due to reaction with residue		No fluorescence		Dull yellowish brown to dull brown fluorescence	Dull yellow to yellowish brown fluorescence	Pale yellow fluorescence (+decrease in fluorescence intensity)			Bright yellow fluorescence	
Hydrogen+Tin(II) Chloride	Morphology	Mineral matter and inert constituents bound together by low relief matrix		Very high relief alginite softens & flows together	Intact Alginite very low relief	Intact Alginite low relief	Intact Alginite moderately low relief	Alginite Morphology unaltered - low relief				
		Coarse-grained tin sulphide aggregates			Abundant aggregates of tin sulphide			Appearance of tin sulphide-abundance and grain size increases with temp.				
	U.V. Light	Matrix material exhibits a very weak brownish fluorescence (?)		Dull yellowish Brown to dull dark brown fluorescence		Dull yellow to yellowish brown fluorescence	Dull greenish yellow to dull yellow fluorescence	Bright pale greenish yellow to bright yellow fluorescence		Bright greenish yellow to yellow fluorescence	Bright pale green to greenish yellow fluorescence	
	Blue Light	Araldite fluorescence due to reaction with residue	No fluorescence	Very dull yellowish brown to brown fluorescence	Dull yellowish brown to brown fluorescence		Yellow fluorescence	Bright yellow fluorescence		Pale yellow fluorescence (decrease in fluorescence intensity)	Bright yellow fluorescence	
Hydrogen+Zinc(II) Chloride	Morphology	Mineral matter and inert constituents bound together by low relief matrix			Alginite softens and flows together to form low relief material	Alginite Morphology unaltered - low relief		Alginite Morphology unaltered - low relief				
	U.V. Light	Matrix material exhibits a very weak brownish fluorescence (?)		No fluorescence	Very weak dark brown fluorescence		Very weak dull yellowish brown to brown fluorescence	Dull yellowish brown to brown fluorescence	Yellow to dull yellowish brown fluorescence	Bright greenish yellow to yellow fluorescence	Bright pale green to greenish yellow fluorescence	
	Blue Light	Araldite fluorescence due to reaction with residue	No fluorescence			Very weak brown fluorescence	Weak brown fluorescence	Weak yellow to yellowish brown fluorescence		Dull yellow	Yellow fluorescence	Bright yellow fluorescence

Table 17: Microanalysis of tars obtained by flash pyrolysis of Tasmanite

Temperature of flash pyrolysis (°C)	506	556	607	653
Carbon (%)	82.0	82.6	82.3	82.2
Hydrogen (%)	10.0	9.4	9.1	8.5
Difference (%)	8.00	8.1	8.6	9.3
Atomic H/C	1.46	1.37	1.33	1.24

5 cm

Fig. 1 X-Ray diffraction traces of demineralized Tasmanite samples

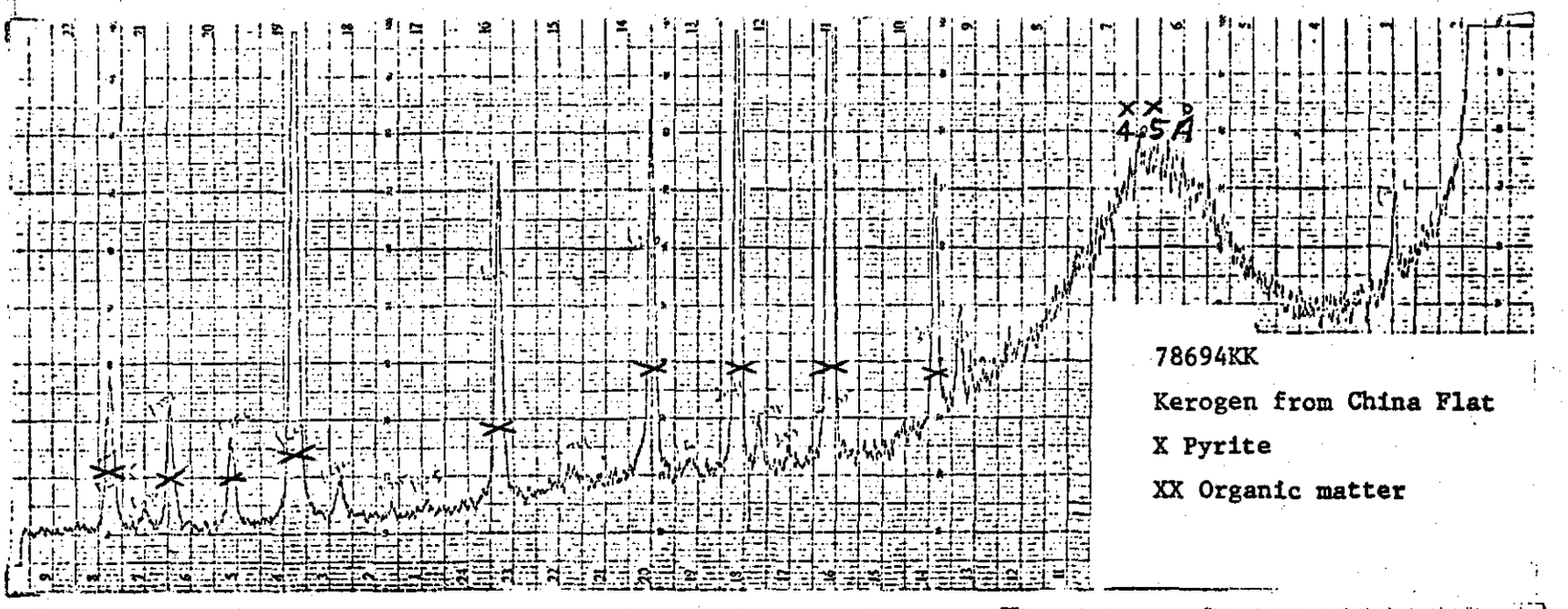

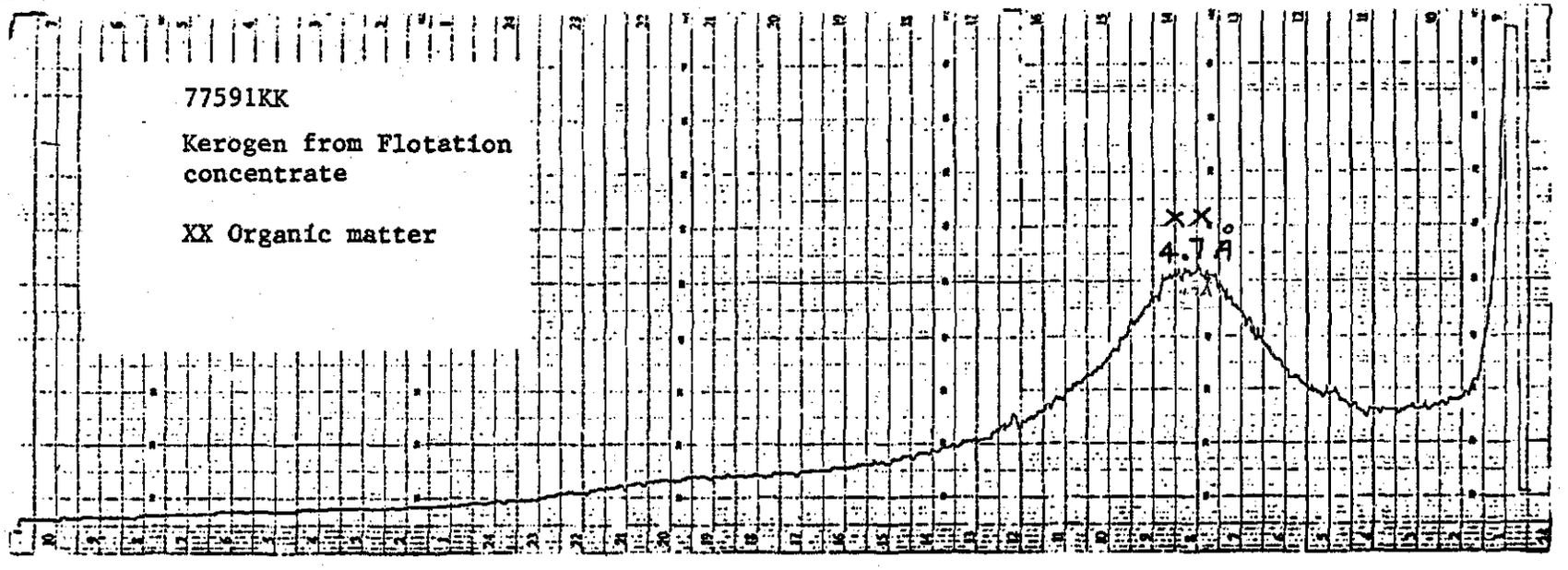

051

146052

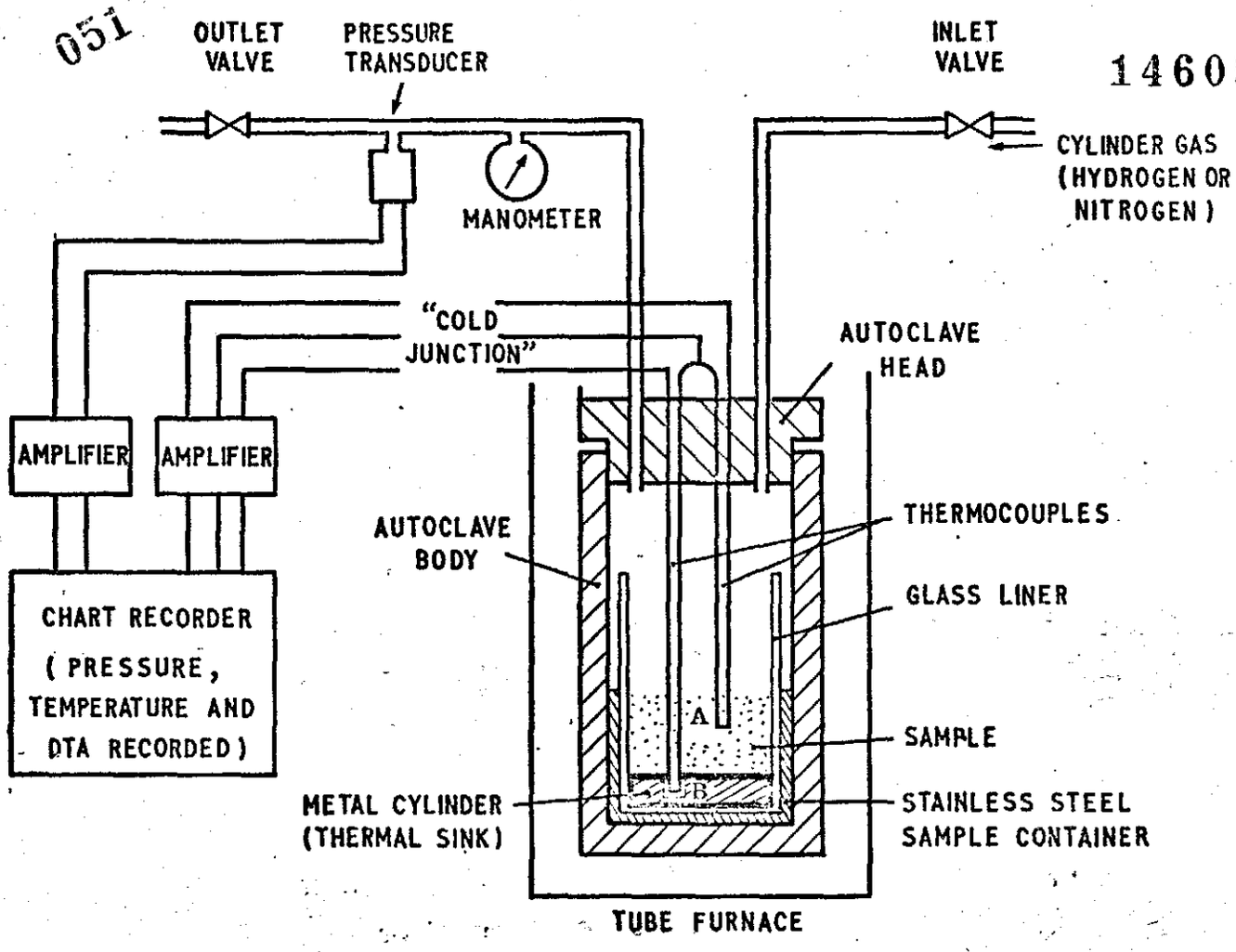

FIGURE 2a AUTOCLAVE ARRANGEMENT FOR HIGH-PRESSURE, SINGLE-CELL, DTA EXPERIMENTS

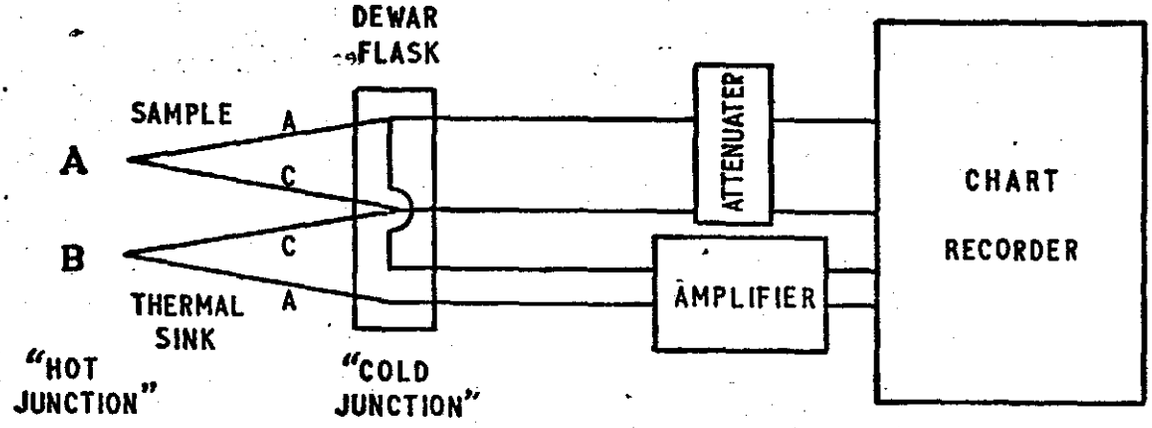

A Chrom-Al Thermocouple in Sample
B Chrom-Al Thermocouple in Metal Cylinder

FIGURE 2b DTA CIRCUIT

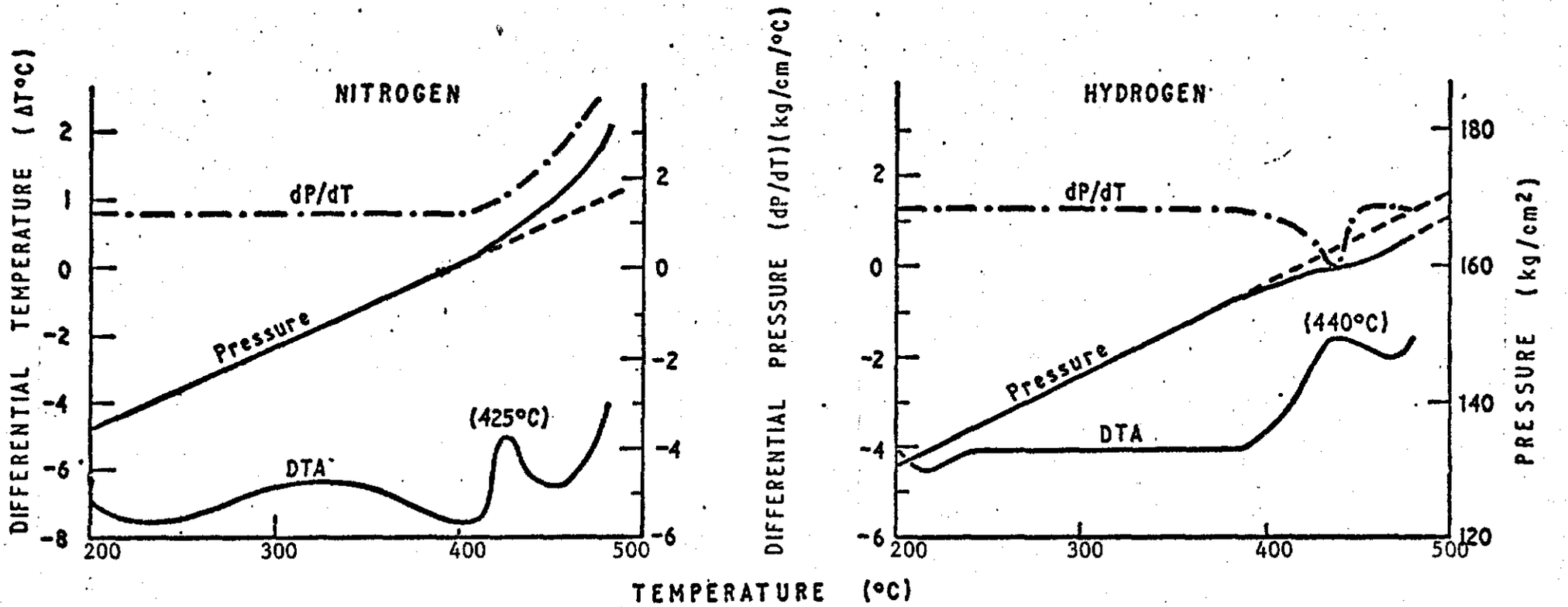

FIGURE 3. DTA, pressure and differential pressure data for the uncatalysed batch autoclave experiments

Note:- temperature of exothermic peaks in parenthesis

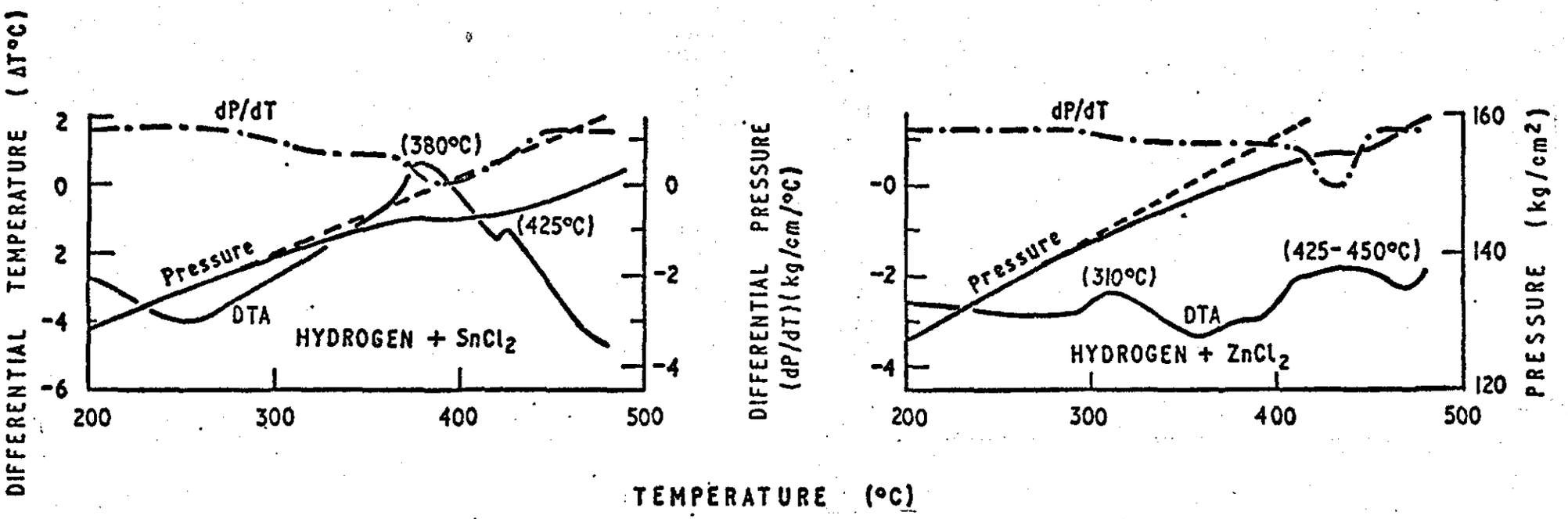

FIGURE 4. DTA, pressure and differential pressure data for the catalysed batch autoclave experiments

Note:- temperature of exothermic peaks in parenthesis

FIGURE 5

The relationship between final pressure and reaction temperature

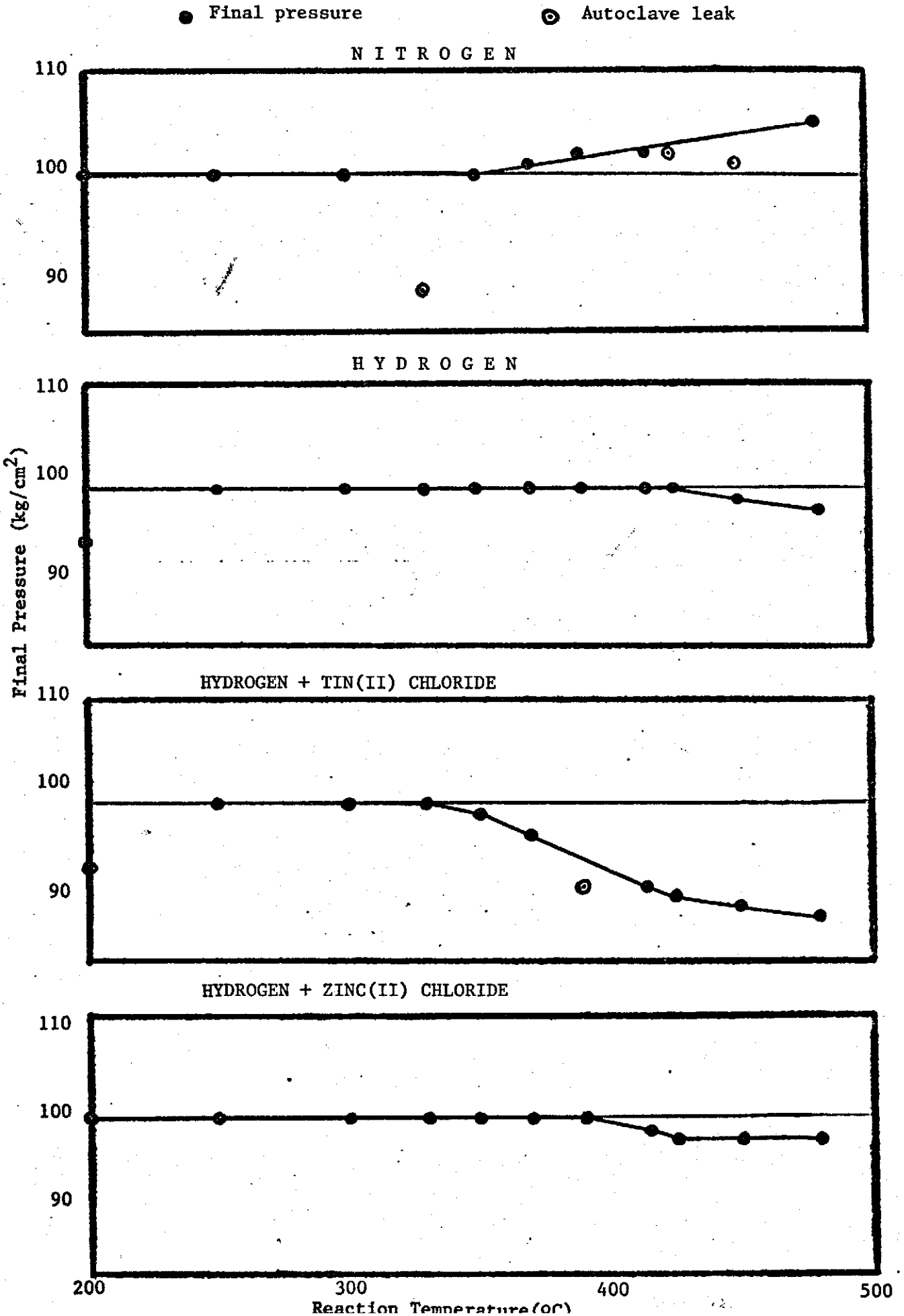

FIGURE 6

The proportion of cylinder gas in the autoclave as a function of the reaction temperature

● 50kg/cm^2 sample ⊙ 20kg/cm^2 sample

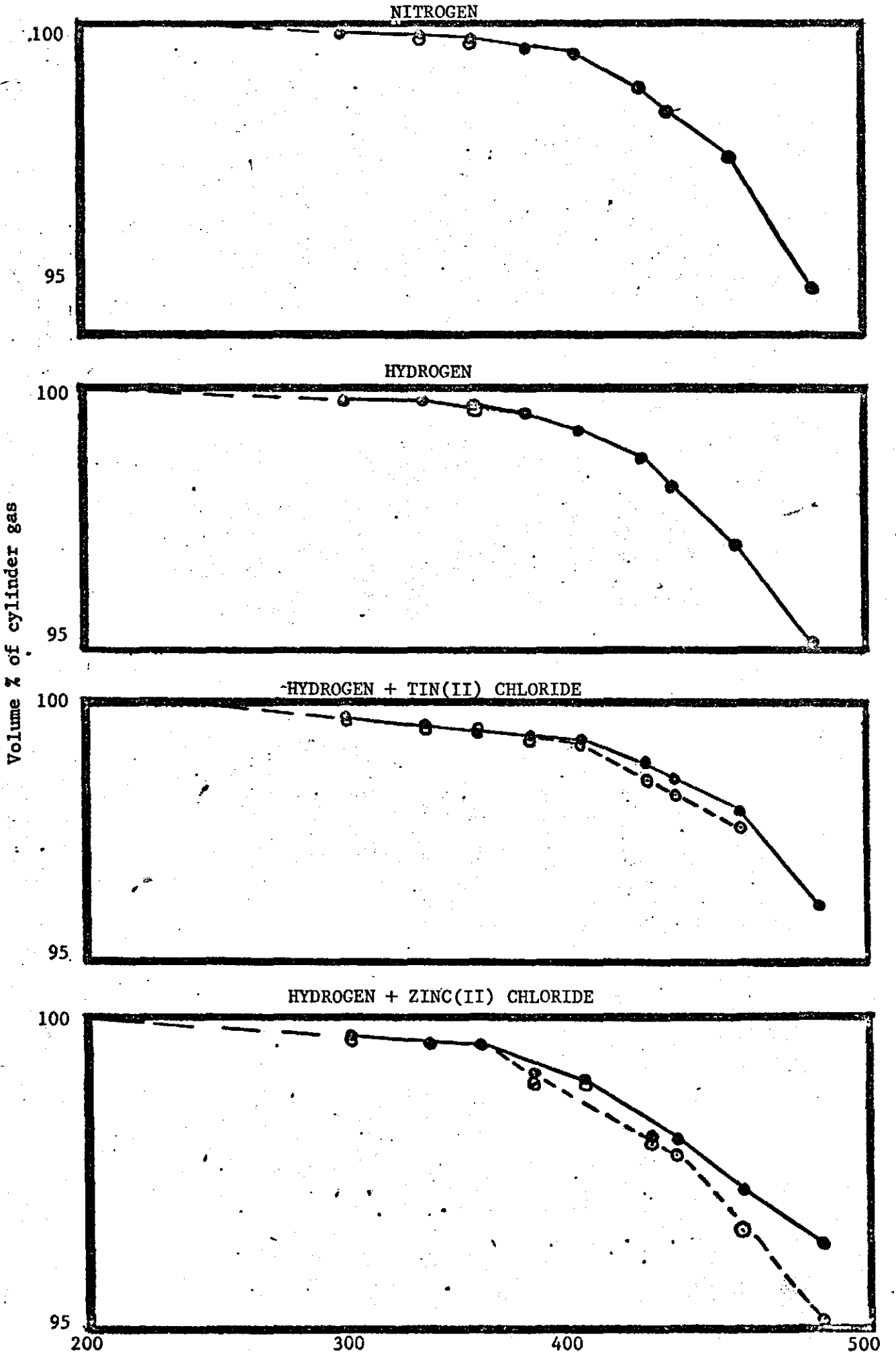

FIGURE 7

The proportions of carbon monoxide, carbon dioxide and hydrocarbons in the autoclave gas sample as a function of the reaction temperature;

(1) the 50kg/cm^2 sample

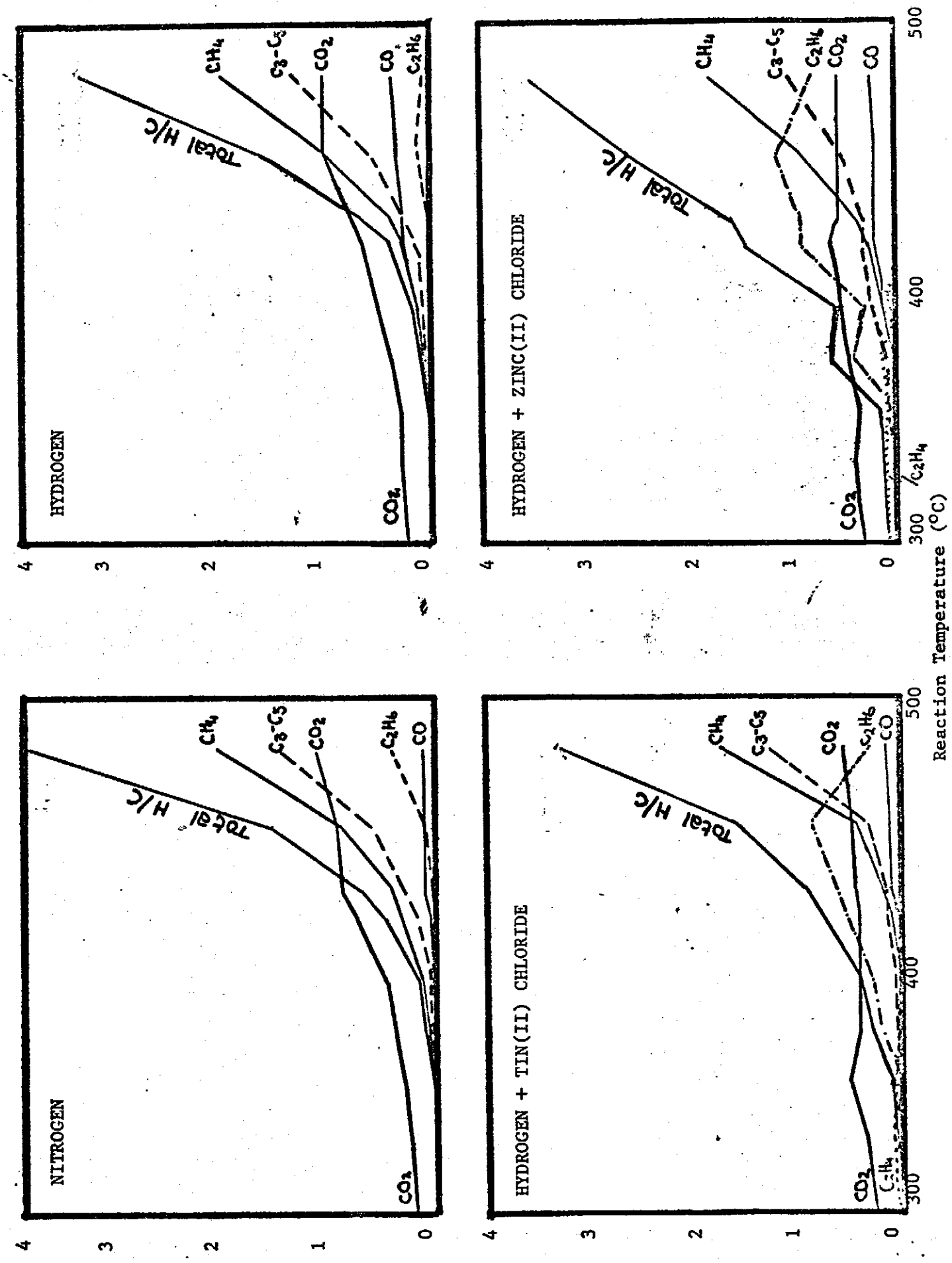

FIGURE 8

146058

057 The proportion of carbon monoxide, carbon dioxide and hydrocarbons in the autoclave gas sample as a function of the reaction temperature; (2) the 20kg/cm^2 sample

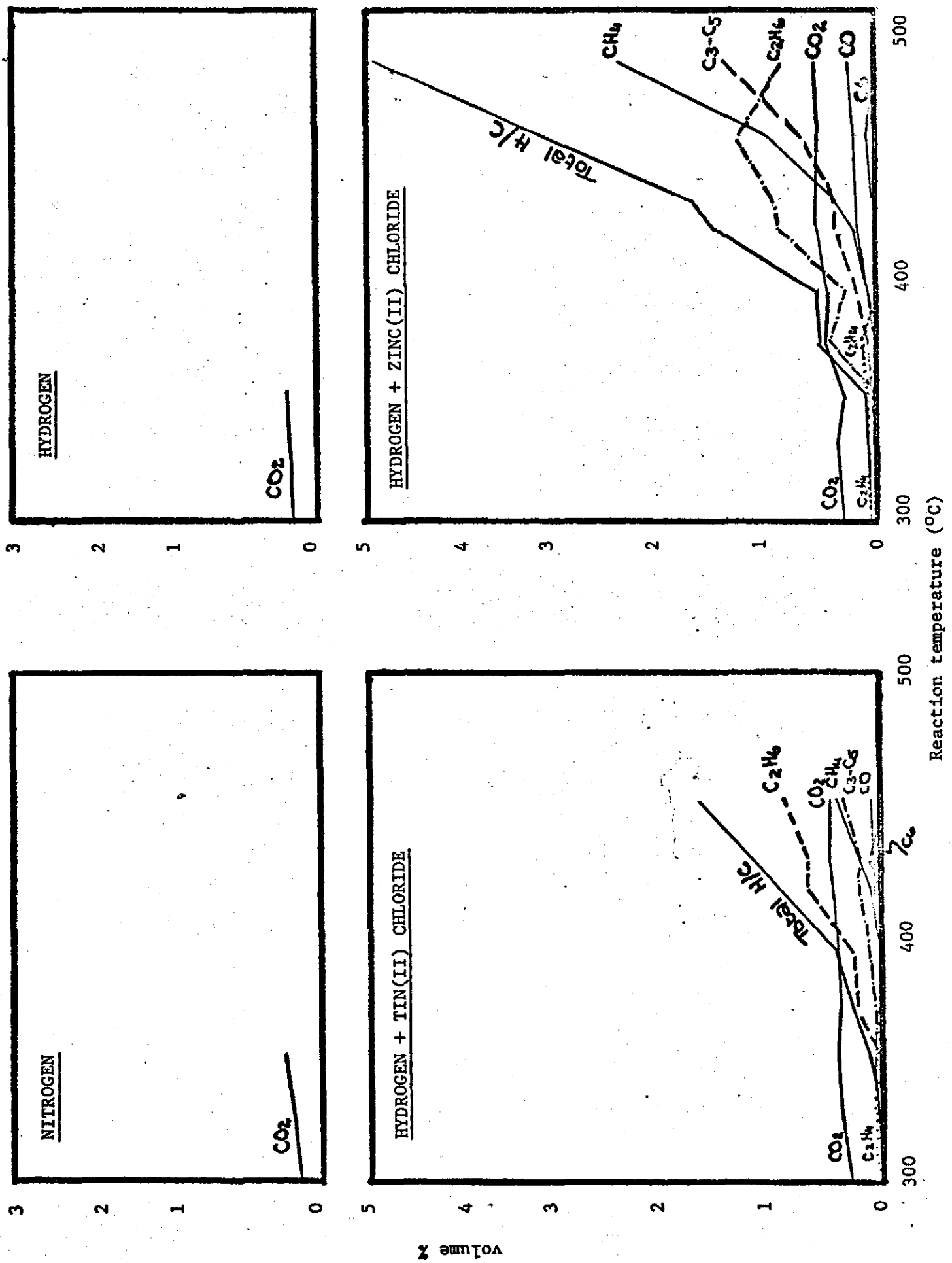

FIGURE 9

The relative proportions of carbon monoxide, carbon dioxide and hydrocarbons; (1) the 50 kg/cm^2 sample

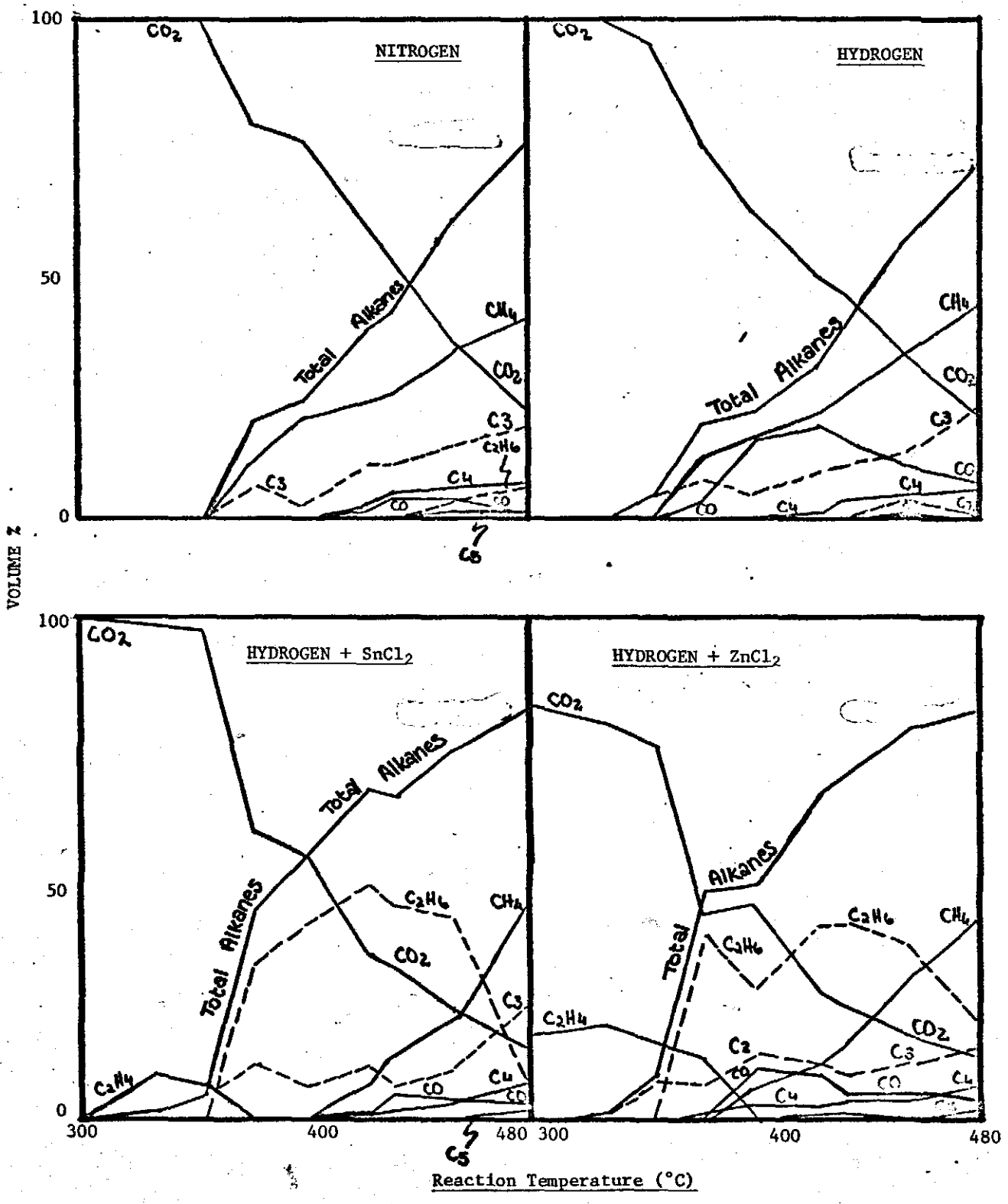

FIGURE 10

The relative proportions of carbon monoxide, carbon dioxide and hydrocarbons; (2) the 20 kg/cm^2 sample

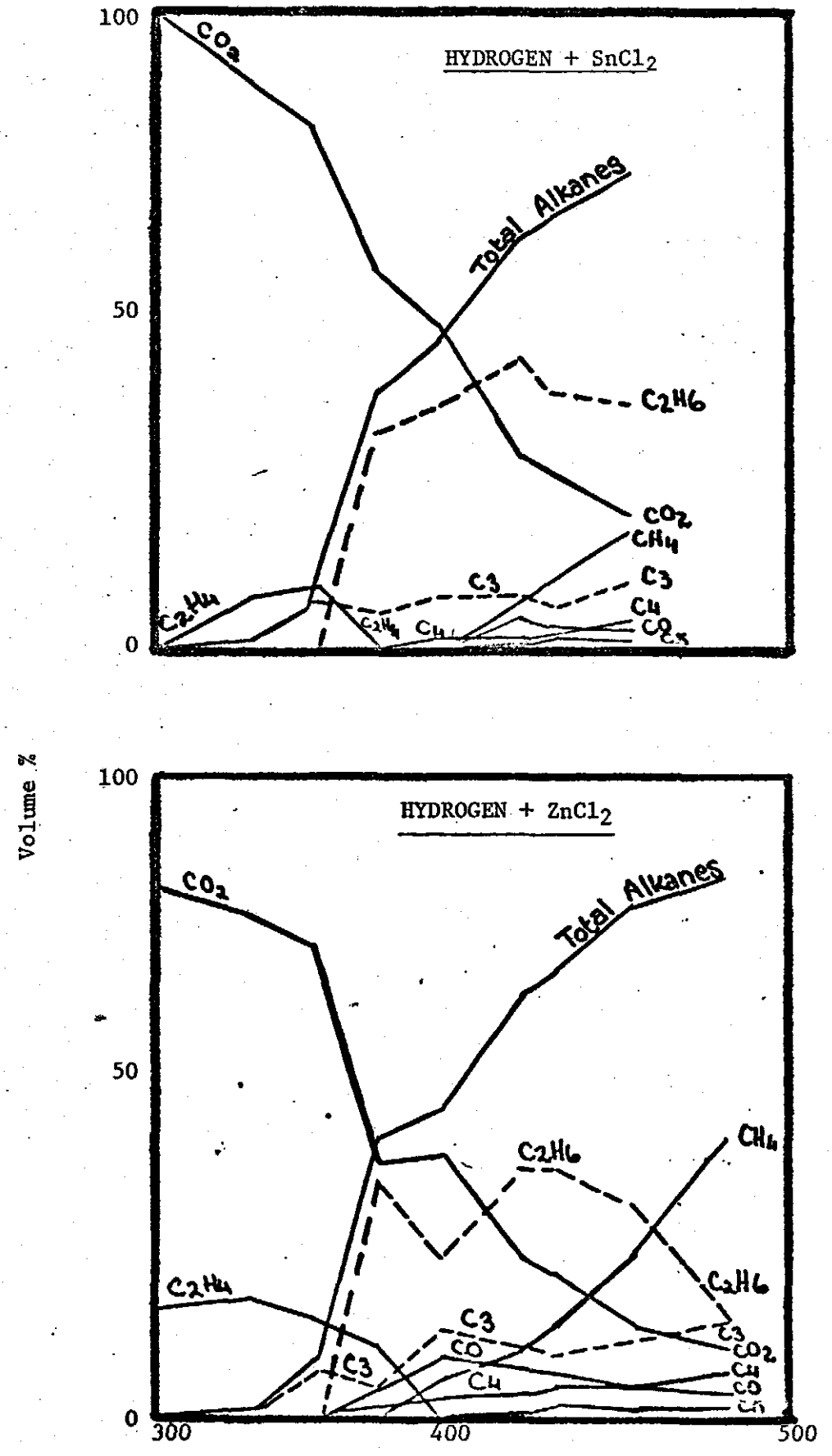

FIGURE 11

Hydrocarbon gas ratios as a function of the reaction temperature

Uncatalysed reactions
..... N_2
-·-·- H_2

Catalysed Reactions
——— $ZnCl_2 + H_2$
– – – $SnCl_2 + H_2$

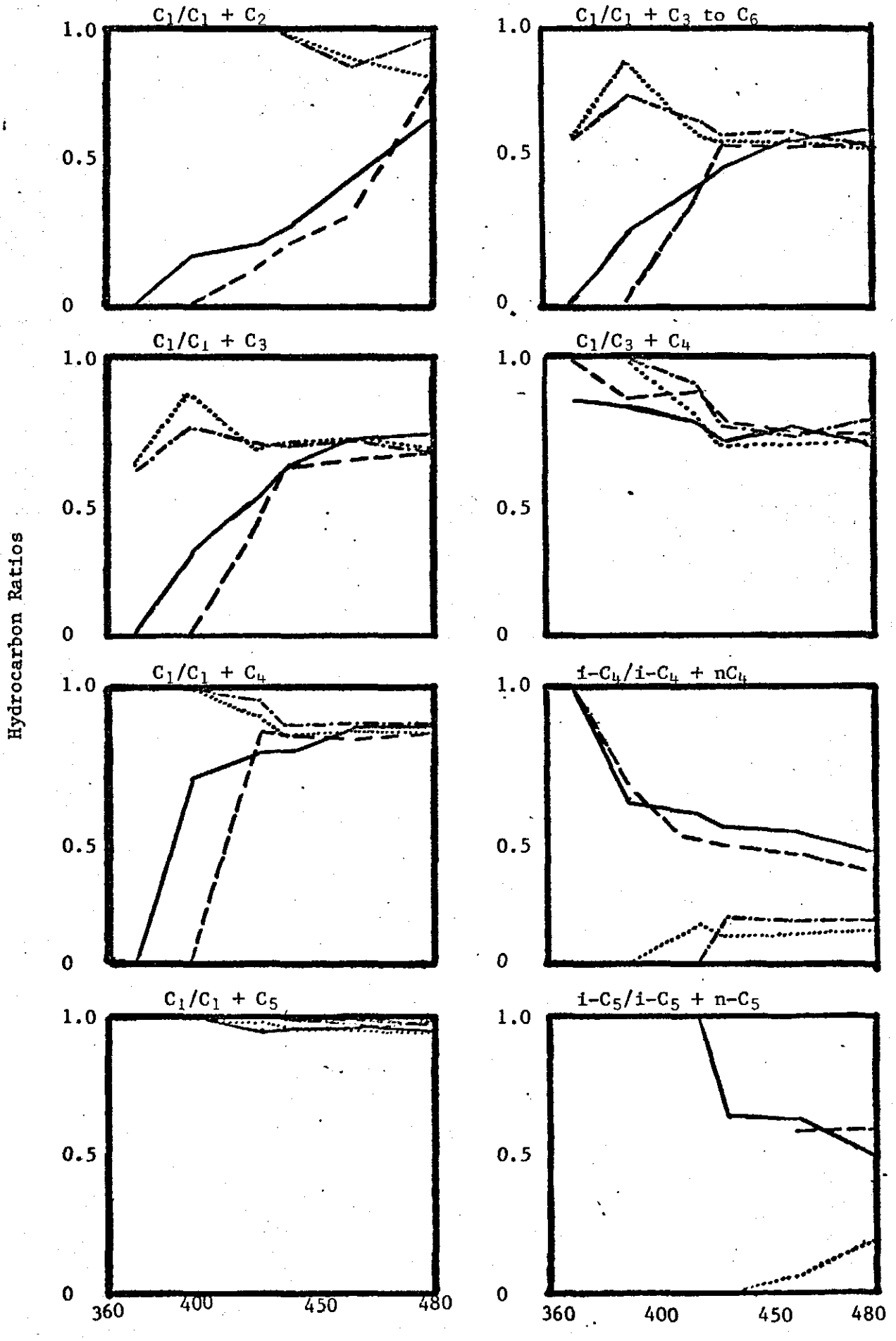

061

FIGURE 12

Conversion of the Tasmanite concentrate to hexane soluble material and heavy hydrocarbons as a function of the reaction temperature

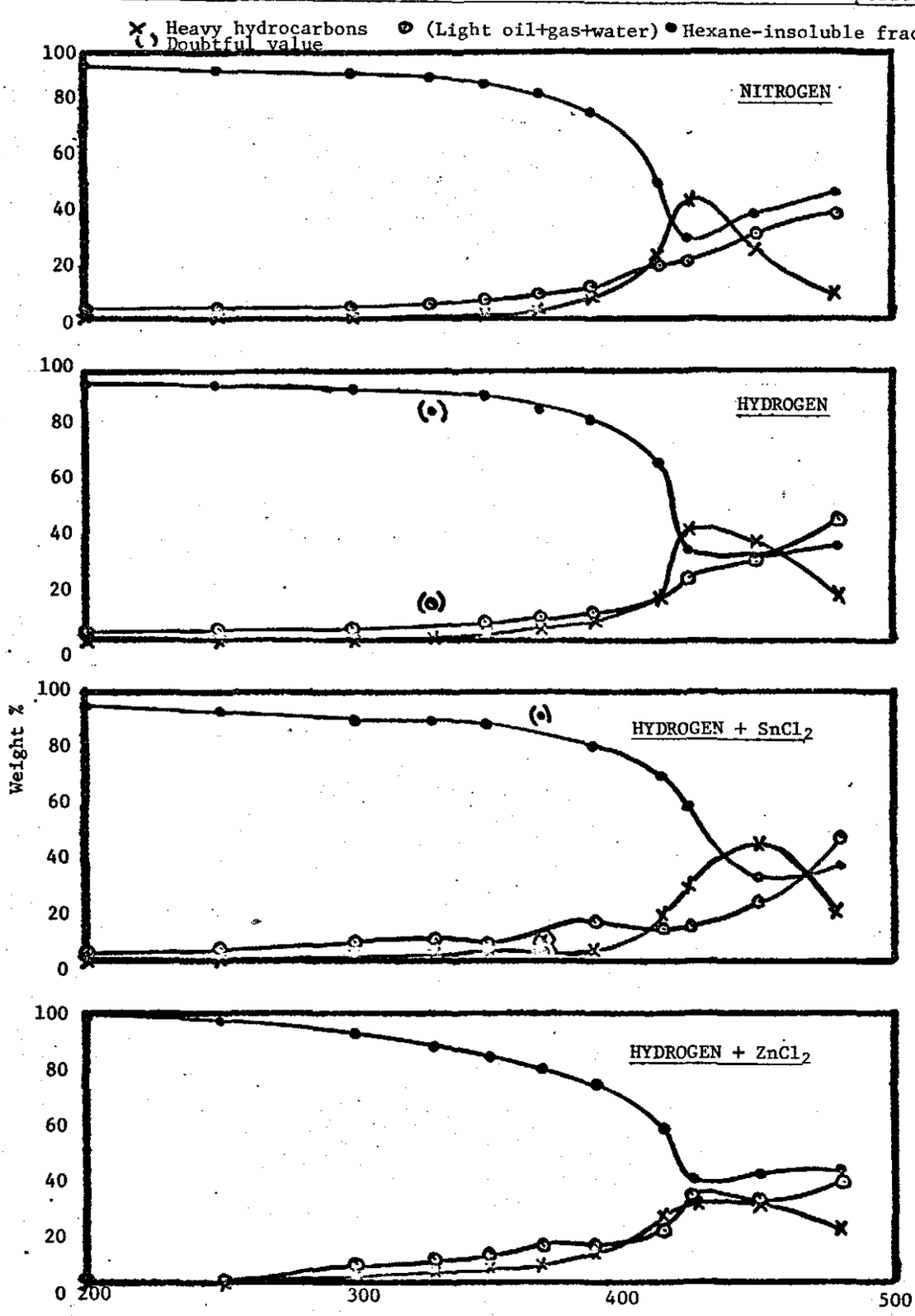

PLATE 1

(INCIDENT LIGHT - AIR OBJECTIVES)

1A Unaltered Tasmanite sp. body exhibiting the characteristic compressed alginite morphology (Nitrogen atmosphere - 200°C) (x 170)

1B As above. Strong intensity fluorescence of alginite in response to blue-light excitation

1C Alginite morphology unchanged apart from very low polishing relief (Nitrogen atmosphere - 390°C) (x 170)

1D As above. Relatively low intensity fluorescence of alginite in response to blue-light excitation

PLATE 1

146064

B

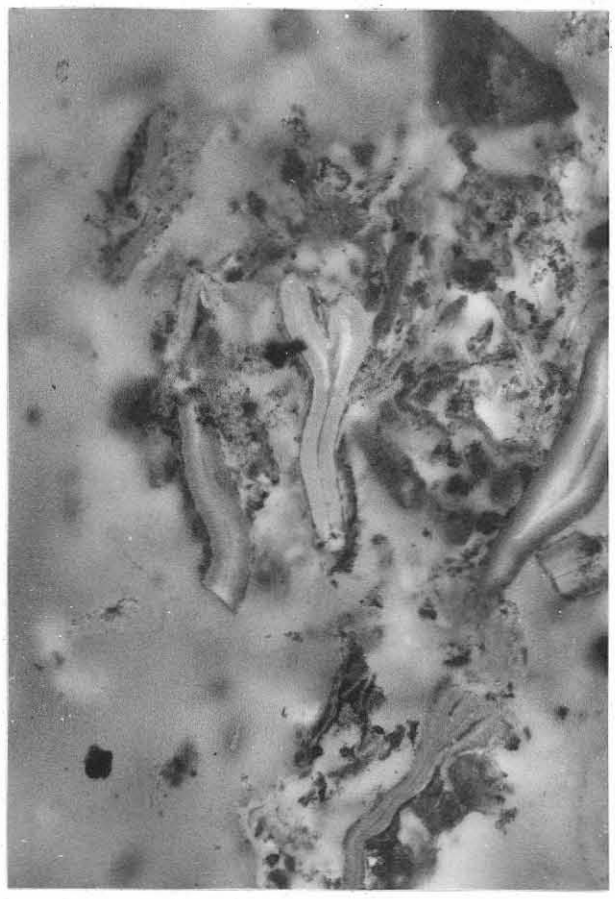

D

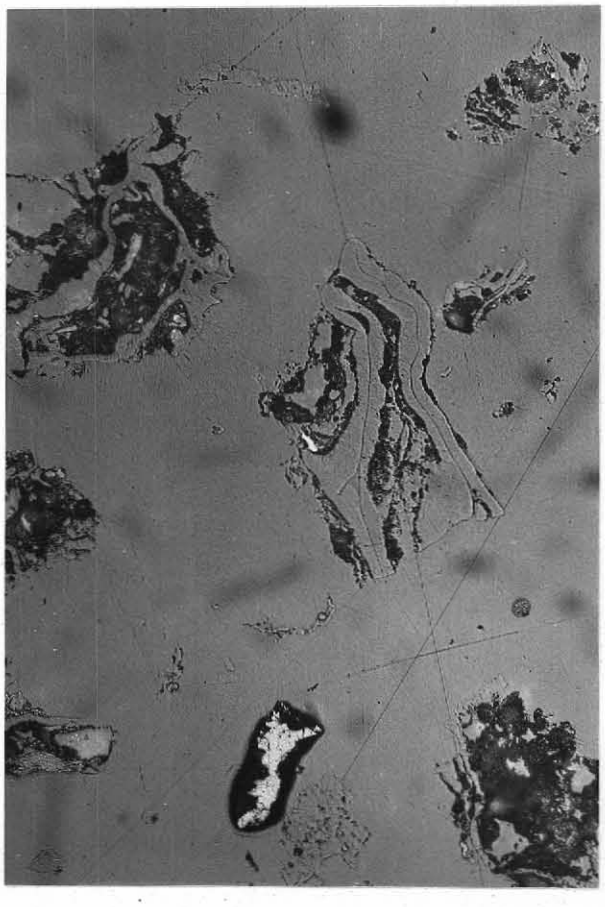

A

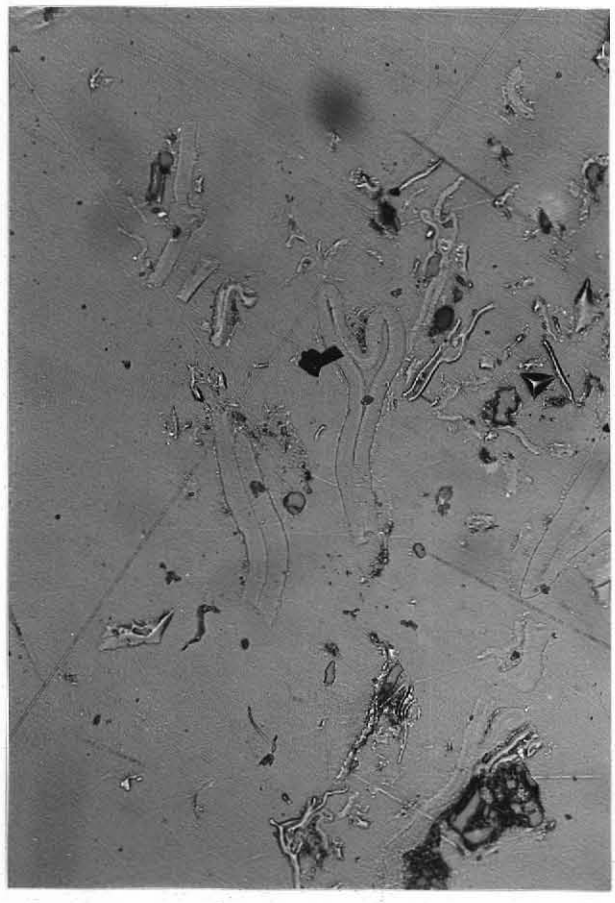

C

PLATE 2

(INCIDENT LIGHT - AIR OBJECTIVES)

2A Alginite surrounded by euhedral/subhedral crystals of tin(II) sulphide (Hydrogen atmosphere + tin(II) chloride - 330°C) (x 170)

2B Alginite associated with tin(II) sulphide crystals. Note the low polishing relief (Hydrogen atmosphere + tin(II) chloride - 350°C) (x 170)

2C Low relief alginite associated with tin(II) sulphide. The latter appears to have developed (in part) inside the alginite (Hydrogen atmosphere + tin(II) chloride - 350°C) (x 170)

2D As above. Moderately strong intensity fluorescence of alginite in response to blue-light excitation

PLATE 2

B

D

A

C

PLATE 3

(INCIDENT LIGHT - AIR OBJECTIVES)

3A Very low relief alginite. The bulk of the alginite having softened and flowed together. (Nitrogen atmosphere - 425°C) (x 170)

3B As above. Detail of "relict" alginite (x 420)

3C Very high relief, carbonized, alginite (Nitrogen atmosphere - 425°C) (x 170)

3D Grains and grain aggregates of euhedral/subhedral tin(II) sulphide and mineral matter (mainly quartz and clay minerals) (Hydrogen atmosphere + tin(II) chloride - 480°C) (x 170)

PLATE 3

B

D

A

C